Hindawi
Journal of Mathematics
Volume 2024, Article ID 2886786, 23 pages
https://doi.org/10.1155/2024/2886786

Research Article

Mathematical Modelling of Host-Pest Interaction in the Presence of Insecticides and Resistance: A Case of Fall Armyworm

Moreen Brenda Gatwiri,[1] **Marilyn Ronoh**,[1] **Cyrus Gitonga Ngari**,[2] **and Dominic Makaa Kitavi**[1]

[1]*Department of Mathematics and Statistics, University of Embu, Embu, Kenya*
[2]*Department of Pure and Applied Sciences, Kirinyaga University, Kerugoya, Kenya*

Correspondence should be addressed to Moreen Brenda Gatwiri; 1414@student.embuni.ac.ke

Received 3 April 2023; Revised 15 October 2023; Accepted 10 November 2023; Published 4 January 2024

Academic Editor: Firdous A. Shah

Several pest management programs have been developed to control rising agricultural pest populations. However, the challenge of rapid evolution and pest resistance towards control measures continues to cause high production losses to maize farmers in Africa. Few models have attempted to address the issue of fall armyworm (FAW) but have barely incorporated the effect of insecticide resistance. Models with resistance would help predict the dynamics of the FAW population, thus mitigating losses. The main objectives of this work were to develop, analyze, and numerically simulate a susceptible-infected deterministic mathematical model expressing the FAW-maize interaction and population dynamics under insecticidal sprays and resistance FAW larvae. Three model steady states are established. Their local stability is conducted using either the eigenvalue or the Routh–Hurwitz stability criteria, and their global stability is analyzed using either the Castillo–Chavez, Perron eigenvector, or the Lyapunov methods. An expression for the basic reproduction number R_0, together with the sensitivity analysis of its parameter values, is provided. Numerical analysis is conducted on various model parameter values. The results established all the model steady states to be locally and globally asymptotically stable at $R_0 \leq 1$. Also, resistance ω increased the infection rates by increasing the FAW larvae survival rate λ and reducing the insecticidal efficacy δ_R and δ_N. This work informs the agriculturists and policymakers on pest control with the best ways to use insecticides to minimize pest resistance and enhance efficacy in production. Pest control measures should be modified to lower the FAW survival rate and all model parameters contributing to resistance formation by FAW larvae to minimize FAW-host interaction, thus reducing crop damage.

1. Introduction

Fall armyworm (FAW), scientifically known as *Spodoptera frugiperda*, is an agricultural pest species of the order Lepidoptera, a larval stage for the fall armyworm moth [1]. It is a polyphagous, sporadic pest that has continuously caused crop destruction and yield losses to both organic and inorganic farmers globally [2]. Maize (corn) is considered a staple food and a source of food security in most African countries; however, farmers continue to face the threat of significant production losses due to climate change, pests, and diseases [3]. Recent research studies show that maize is the most preferred host plant of FAW [4]. Various integrated control mechanisms for both organic and inorganic maize farming have been put in place to control the pest-host (FAW-maize) interactions, but natural selection and mutation have caused FAW resistance towards set control mechanisms [5].

Recent studies show that improperly managed FAW invasion in a maize plantation can cause a significant reduction in the quality and quantity of the harvest [6]. In Africa, the conducive weather conditions and the availability of FAW-preferred host favor rapid FAW reproduction. This makes FAW the most dominant and endemic pest in Africa and thus a great threat to production and food security [7]. Synthetic insecticides are the main control methods adopted

globally against FAW pest invasions, especially in Africa where governments are spending huge funds buying and distributing insecticides to their farmers [8]. However, continuous use of the insecticides increases the chances of pest resistance against the control method and thus high production cost [9, 10].

With maize being a staple food in Kenya and also FAW's most preferred host plant [6], the negative impacts of FAW on maize production significantly affect Kenya's Big Four Agenda of achieving 100% national nutrition and food security and the entire African economic developments [11]. The poor-quality maize yields negatively affect the country's GDP due to poor market access [12]. Managing FAW populations is also expensive for most undeveloped African countries. Generally, FAW's invasion of the agricultural sector in Africa poses a great threat to the achievement of the CAADP Malabo Declaration of halving poverty by 2025 and the achievements of the 2030 Sustainable Development Goals (SDGs) of improving food security, eradicating poverty, and achieving sustainable production and consumption plans [7, 12].

Predicting the dynamics of a pest population and evaluating the existing pest control measures could significantly reduce the number and the cost of pest management, thus improving crop production, food security, and sustainability [13]. There is an increased need to study FAW-maize interaction and the application of insecticides with the evolution of resistance to develop better control methods that are more efficient, effective, and economical [12, 14]. Mathematical modeling offers an avenue to explore such important factors in agricultural production [15]. For instance, crop growth models issue physiological approaches for the simulations of pest destructions and crop interactions [16].

The disease infection rate in the maize population could be decreased through control intervention measures such as chemical insecticides aimed at reducing susceptible-infected maize contact rates [17]. In the present work, we will consider chemical insecticides as the major control method against FAW. However, resistance alleles and migration rates significantly influence FAW population dynamics [18]. Ordinary differential equations (ODEs) have been used in developing and analyzing stage-structured FAW-maize interaction models [13, 17–19]. However, limited attention has been paid to host-pest interaction models, particularly in insect pest management measures [20]. Thus, we apply ODEs and the concept of host-pest interaction models to study FAW larvae population dynamics in maize populations.

From the literature, various deterministic mathematical models describing the dynamics of agricultural pest populations under various pest control measures have been developed [17–19, 21–24]. Moreover, mathematical models evaluating the effects of pests and insecticides on crop production have been developed [13, 25]. However, despite many pest control models in agricultural production, comprehensive parametric research is limited. Also, limited host-pest interaction models address various pest management measures. From the previous studies of models on agricultural pests, we did not find a mathematical model on the host-pest (FAW-maize) interaction assessing the interaction and population dynamics under an insecticidal control strategy. Through natural selection and mutation, a proportion of FAW pests are considered to express resistance traits against insecticides, thus increasing the host-pest interactions and reducing the insecticide's efficacy [5].

To address this gap, this study develops a susceptible-infected (SI) compartmental model for two interacting populations, FAW-maize population, assessing the effects of insecticide sprays and resistance factors on the interaction patterns and population dynamics. SI models are used to model the rate and transmission dynamics of infectious human or plant diseases [26, 27]. This study assumes that the FAW larvae depend largely on the maize population for food and survival and considers insecticides which are the most commonly used control methods against FAW. This research study will increase the understanding of the fall armyworm-maize interaction patterns and the best control measures to employ when the FAW species is in its larval stage while minimizing larvae resistance formation. This will significantly improve on crop production enhancing food security and economic development [28].

A study by Daudi 2021 proposed a stage-structured model for the control of FAW impacts on maize production. Two interacting maize-FAW submodels were developed with the maize population divided into two stages: vegetative $X_1(t)$ and reproductive $X_2(t)$ stages, while the FAW population was divided into three stages, that is, the egg $E(t)$, caterpillar $C(t)$, and adult $A(t)$ stages. In this study, we introduce the knowledge of epidemiological disease models to model the population dynamics of maize-FAW interaction. We develop a susceptible-infected (SI) compartmental model for two interacting populations: the maize population and the FAW population as shown in (Figure 1). In SI models, infection occurs when a susceptible individual comes into contact with an infected individual, thus contracting the disease [29]. The FAW larvae infect the susceptible maize population after making contact. We introduce two factors: FAW control through insecticides and resistance, as important factors affecting the interaction patterns, the spread of the disease, and the model population dynamics. The model is analyzed, and numerical simulation is conducted using the MATLAB ODE solver with the data obtained from previously published articles cited accordingly in this work.

2. Model Description and Formulation

In formulating the maize-FAW SI model shown in Figure 1, we consider two maize sections: organic (O) and insecticidal (I). The organic section (O) is without any FAW control methods, while the insecticidal section (I) is under insecticidal spraying. The FAW larvae $N_L(t)$ infect the maize population $N_M(t)$ through contact. The FAW larvae population has been divided into two compartmental classes, that is, the normal larval $L_N(t)$ and the resistant larval $L_R(t)$

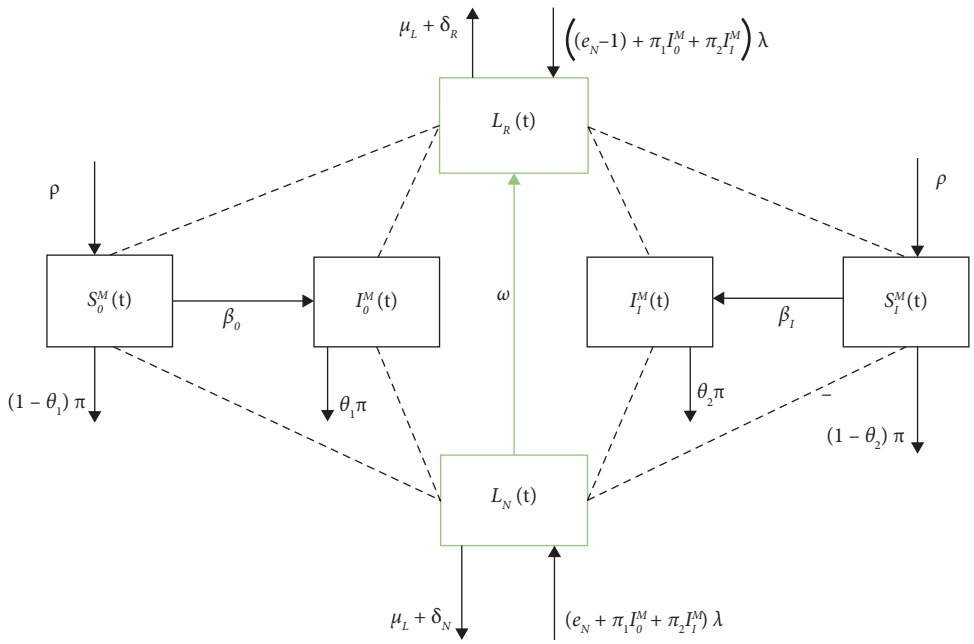

Figure 1: A flow diagram for the FAW larvae-maize interaction model.

populations. A proportion of normal larvae progress into resistance larvae at a constant rate ω after contact with insecticides. The two maize sections interact naturally with both the normal larvae $L_N(t)$ and the resistant larvae $L_R(t)$. The maize population transits from the susceptible into the infected compartmental class after making contact with either the resistant or the normal larvae that transmit the disease. The maize population in the two sections then progresses from susceptible $S^M(t)$ into the infected $I^M(t)$ compartments through two forces of infection β_O and β_I. Susceptible and infected maize populations at any time t in the organic section (O) are denoted as $S_O^M(t)$ and $I_O^M(t)$, respectively, while the susceptible and infected maize populations at any time t in the insecticidal section (I) are denoted as $S_I^M(t)$ and $I_I^M(t)$, respectively.

The natural recruitment rates of the maize population occur at a constant rate ρ. The natural recruitment rate contributing to the FAW larvae population is a constant rate e_N through a survival rate λ. The FAW population $N_L(t)$ slowly kills the host maize population $N_M(t)$ by residing in it, infecting and feeding on the maize biomass [13]. This contributes to an increased recruitment rate of FAW at a rate (π_1, π_2) and a reduction in the maize population over time. The natural harvesting rate of the maize population is a constant rate denoted by π. The FAW larvae population declines at a constant rate $\mu_L = \mu_1 + \mu_2$ which is either by the natural death rate μ_1 or progression into the pupal FAW life cycle at a constant rate μ_2. The exposure to insecticides causes death of the FAW larvae at constants rates δ, with δ_N denoting the normal larvae insecticidal-induced death rate and δ_R denoting the resistance larvae insecticidal-induced death rate, with $\delta_N < \delta_R$.

The total population in the model at time t will be$N(t) = N_L(t) + N_M(t)$, where $N_L(t) = L_N(t) + L_R(t)$.

$N_M(t) = S_O^M(t) + I_O^M(t) + S_I^M(t) + I_I^M(t)$.

The infection force at any time t in the organic section (O) is denoted as β_O and that in the insecticidal section (I) is denoted as β_I:

$$\beta_O = \eta_O\left(\frac{L_N + \varepsilon L_R}{N_M}\right),$$
$$\beta_I = \eta_I\left(\frac{L_N + \varepsilon L_R}{N_M}\right), \tag{1}$$

where $\beta_O > \beta_I$ and $0 < \beta_O, \beta_I < 1$, $0 < \varepsilon < 1$, and infection rates $\eta_0 > \eta_1$.

In this study, the following assumptions were made during model formulation:

(1) To reduce model complexity, the model only considers one larvae stage of the FAW life cycle. The other FAW stages are represented by the FAW recruitment rate e_N and progression rate μ_2.

(2) FAW larvae $N_L(t)$ are the only pest interacting with the maize population at time t.

(3) Insecticidal sprays are the only control methods adopted against the FAW population.

(4) The term normal larvae denote the larvae not expressing the resistance traits.

(5) The immigration and emigration rates of the adult FAW larvae population are considered to be negligible.

(6) The model assumes homogenous mixing of the FAW and maize population at any time t.

The following state variables in Table 1 and model parameters in Table 2 are discussed as used in model formulation.

Considering the state variables, parameters, and assumptions discussed above, we developed the model flowchart diagram given in Figure 1.

Table 1: A description of the model state variables.

State variable	Description
$S_O^M(t)$	Susceptible maize population in the organic section at any time t
$I_O^M(t)$	Infected maize population in the organic section at any time t
$S_I^M(t)$	Susceptible maize population in the insecticidal section at any time t
$I_I^M(t)$	Infected maize population in the insecticidal section at any time t
$L_N(t)$	Normal larvae population at any time t
$L_R(t)$	Resistant larvae population at any time t

Table 2: A description of model parameters.

Model parameter	Description
β	The force of infection from susceptible to infected maize population
θ_1	The harvesting rate of organic maize population $N_O^M(t)$
θ_2	The harvesting rate of insecticidal sprayed maize population $N_I^M(t)$
η_0	The infection rate in β_0
η_1	The infection rate in β_1
e_N	The natural recruitment rate of $N_L(t)$ from the naturally occurring FAW population
π	The lost maize biomass in $N_M(t)$ at any time t due to caterpillar attack
ω	The rate at which normal larvae progress into the resistance larvae population
ρ	The natural recruitment rate of maize biomass into the maize population
μ_L	The total population decrease rate of $N_L(t)$ at time t
μ_2	The progression rate to the pupal FAW life cycle
μ_1	The natural death rate of the FAW larvae at any time t
δ	The insecticidal-induced death rate in the $N_L(t)$ population
λ	The survival rate of $L_N(t)$ and $L_R(t)$ from the egg stage of the FAW population at any time t
π_1, π_2	The maize biomass from the $I_O^M(t)$ and $I_I^M(t)$ classes, respectively, contributing directly to the $N_F(t)$ classes increased the natural recruitment rate

The system of ordinary differential equations governing the interaction of Fall Armyworm larvae with maize is given by the following equations:

$$\frac{dS_O^M}{dt} = \rho - \beta_O S_O^M - (1-\theta_1)\pi S_O^M, \tag{2}$$

$$\frac{dI_O^M}{dt} = \beta_O S_O^M - \theta_1 \pi I_O^M, \tag{3}$$

$$\frac{dS_I^M}{dt} = \rho - (1-\theta_2)\pi S_I^M - \beta_I S_I^M, \tag{4}$$

$$\frac{dI_I^M}{dt} = \beta_I S_I^M - \theta_2 \pi I_I^M, \tag{5}$$

$$\frac{dL_N}{dt} = \lambda\left(e_N + \pi_1 I_O^M + \pi_2 I_I^M\right) - (\omega + \mu_L + \delta_N)L_N, \tag{6}$$

$$\frac{dL_R}{dt} = \left((1-e_N) + \pi_1 I_O^M + \pi_2 I_I^M\right)\lambda + \omega L_N - (\mu_L + \delta_R)L_R. \tag{7}$$

3. Model Analysis

3.1. Positivity of Solutions. Positivity ensures that the model is well-posed and the equations lie on the feasible region of the system and thus realistic in representing pest-host interaction with positive values [30]. Since the model system describes a living population of the FAW larvae-maize interaction, then the state variables and the model parameters are positive at any time $t > 0$. We prove the positivity of solutions of our model system shown in Figure 1 by stating and proving Theorem 1 below [31].

Theorem 1. *Let the initial dataset be* $\{S_O^M(0), I_O^M(0), S_I^M(0), I_I^M(0), L_N(0), \text{and } L_R(0) \geq 0\} \epsilon\, \Omega\, \epsilon\, R_+^6$. *Then, the solution set* $S_O^M(t), I_O^M(t), S_I^M(t), I_I^M(t), L_N(t), \text{and } L_R(t)$ *is positive for all* $t \geq 0$.

Proof. Let the variables $S_O^M(t), I_O^M(t), S_I^M(t), I_I^M(t), L_N(t)$, and $L_R(t)$ be solutions to the system of nonnegative initial conditions:

$$S_O^M(t) \geq 0, I_O^M(t) \geq 0, S_I^M(t) \geq 0, I_I^M(t) \geq 0, L_N(t) \geq 0 \text{ and } L_R(t) \geq 0. \tag{8}$$

Starting with equation (1),

$$\frac{dS_O^M}{dt} = \rho - \beta_O S_O^M - (1-\theta_1)\pi S_O^M. \tag{9}$$

Clearly, by the inspection method, $\rho \geq 0$ on the assumption of nonnegative model variables and parameters.

We need to show that

$$\begin{aligned} \frac{dS_O^M}{dt} &\geq -\beta_O S_O^M - (1-\theta_1)\pi S_O^M, \\ \frac{dS_O^M}{dt} &\geq -(\beta_O + (1-\theta_1)\pi) S_O^M. \end{aligned} \tag{10}$$

By separation of variables, we obtain

$$\frac{dS_O^M}{S_O^M} \geq -(\beta_O + (1-\theta_1)\pi)dt. \tag{11}$$

Upon integration with respect to time (t), $S_O^M(t) \geq C_1 e^{-(\beta_O + (1-\theta_1)\pi)t}$ where C_1 is a constant of integration at $t = 0$.

That is, $C_1 = S_O^M(0)$.

Thus,

$$S_O^M(t) \geq S_O^M(0) e^{-(\beta_O + (1-\theta_1)\pi)t} \geq 0. \tag{12}$$

Hence, the first equation is positive.

By applying the same procedure, we obtain

$$\begin{aligned} I_O^M(t) &\geq I_O^M(0) e^{-\theta_1 \pi t} \geq 0, \\ S_I^M(t) &\geq S_I^M(0) e^{-((1-\theta_2)\pi + \beta_I)t} \geq 0, \\ I_I^M(t) &\geq I_I^M(0) e^{-\theta_2 \pi t} \geq 0, \\ L_N(t) &\geq L_N(0) e^{-(\omega + \mu_L + \delta_N)t} \geq 0, \\ L_R(t) &\geq L_R(0) e^{-(\mu_L + \delta_R)t} \geq 0. \end{aligned} \tag{13}$$

Hence, the solution set $\{S_O^M(t), I_O^M(t), S_I^M(t), I_I^M(t), L_N(t), \text{and } L_R(t)\}$ for the model system is proved to be positive at all $t \geq 0$. Hence, the model equations lie in the feasible region. □

3.2. Boundedness/Invariant Region. To prove for boundedness of the solution of our model system, we state and prove the following theorem as applied by [32].

Theorem 2. *The solution to the study model equations in Section 2 is uniformly bounded in a proper subset* $\Omega = \Omega_M \chi \Omega_f$ *such that* $\Omega = \Omega_M$. $\Omega_f = \{S_O^M, I_O^M, S_I^M, I_I^M, L_N, L_R \in R_+^6 |\ N_M \leq \widetilde{\rho}/\widetilde{\pi}, N_L \leq \widetilde{\lambda}/\widetilde{\delta}\}$.

With $\Omega_M = \{S_O^M, I_O^M, S_I^M, I_I^M \epsilon R_+^4 | N_M \leq \widetilde{\rho}/\widetilde{\pi}\}$ and $\Omega_f = \left\{L_N, L_R \in R_+^2 | N_L \leq \widetilde{\lambda}/\widetilde{\delta}\right\}$, then all the solutions to the model system move into and remain in Ω.

Proof. To get the boundedness of the solution for the maize population at any time t, we take the time derivative of our total maize population along its solution to get

$$\begin{aligned} N_M(t) &= S_O^M(t) + I_O^M(t) + S_I^M(t) + I_I^M(t), \\ \frac{dN_m}{dt} &= \rho - (1-\theta_1)\pi S_O^M - \theta_1 \pi I_O^M + \rho - (1-\theta_2)\pi S_O^M - \theta_2 \pi I_I^M, \\ \frac{dN_m}{dt} &= (\rho + \rho) - \pi\left(S_O^M + S_I^M\right) - \pi\left(\theta_1 S_O^M + \theta_2 S_I^M\right) - \pi\left(\theta_1 I_O^M + \theta_2 I_I^M\right) \leq \widetilde{\rho} - \widetilde{\pi} N_M \\ &\Longrightarrow \frac{dN_M}{dt} \leq \widetilde{\rho} - \widetilde{\pi} N_M, \end{aligned} \tag{14}$$

where $\widetilde{\rho} = (\rho + \rho)$ and $\widetilde{\pi} N_M = \pi(S_O^M + S_I^M) + \pi\ (\theta_1 S_O^M + \theta_2 S_I^M) + \pi(\theta_1 I_O^M + \theta_2 I_I^M)$.

Next, we need to show that every solution originating from Ω stays in Ω and is bounded by $\Omega_M \times \Omega_f$. Consider Lemma 3 [33] stated below. □

Lemma 3. *The linear differential equation* $(dN_M/dt) \leq \widetilde{\rho} - \widetilde{\pi} N_M$, *where* $a = \widetilde{\pi} \neq 0$ *and* $b = \widetilde{\rho}$ *are constants, has infinitely many solutions labeled by* $c \epsilon R$ *as*

$$N_M(t) \leq \frac{\widetilde{\rho}}{\widetilde{\pi}} + N_M(0) e^{-\widetilde{\pi} t}. \tag{15}$$

Proof. $N_M{}'(t) - \widetilde{\pi} N_M(t) \leq \widetilde{\rho}$ is also denoted as $N_M{}' - \widetilde{\pi} N_M \leq \widetilde{\rho}$.

Introducing an integrating factor μ, we get $\mu N_M{}' - \mu \widetilde{\pi} N_M \leq \mu \widetilde{\rho}$.

Let $-\mu\widetilde{\pi} = \mu'$, and thus, $\mu N_M{}' + \mu' N_M \leq \mu \widetilde{\rho}$.

The left-hand side can be expressed as a total derivative of a product of two functions:

$$(\mu N_M)' \leq \mu\widetilde{\rho}. \tag{16}$$

Replacing the value $\mu = e^{\widetilde{\pi}t}$ in the equation above, we obtain

$$\begin{gathered}\left(e^{\widetilde{\pi}t}N_M\right)' \leq e^{\widetilde{\pi}t}\widetilde{\rho}, \left(e^{\widetilde{\pi}t}N_M\right)' \leq \left(\frac{1}{\widetilde{\pi}}e^{\widetilde{\pi}t}\widetilde{\rho}\right)', \\ \left(\left(N_M - \frac{\widetilde{\rho}}{\widetilde{\pi}}\right)e^{\widetilde{\pi}t}\right)' \leq 0.\end{gathered} \tag{17}$$

Upon integration,

$$\begin{gathered}\left(\left(N_M - \frac{\widetilde{\rho}}{\widetilde{\pi}}\right)e^{\widetilde{\pi}t}\right) \leq N_M(0), \\ N_M(t) \leq \frac{\widetilde{\rho}}{\widetilde{\pi}} + N_M(0)e^{-\widetilde{\pi}t},\end{gathered} \tag{18}$$

$\lim_{t\longrightarrow\infty} N_m(t) \leq \widetilde{\rho}/\widetilde{\pi}$, and thus, as $t \longrightarrow \infty$, we have $N_M(t) \leq \widetilde{\rho}/\widetilde{\pi}$.

Similarly, for the FAW larvae population,

$$\begin{gathered}\frac{\mathrm{dN}_L}{\mathrm{d}t} = \lambda + \lambda\pi_1 I_O^M + \lambda\pi_2 I_I^M + \lambda\pi_1 I_O^M + \lambda\pi_2 I_I^M - \mu_L L_N - \mu_L L_R - \delta_N L_N - \delta_R L_R, \\ \frac{\mathrm{dN}_L}{\mathrm{d}t} \leq \widetilde{\lambda} - \widetilde{\delta}N_L,\end{gathered} \tag{19}$$

where $\widetilde{\lambda} = \lambda + \lambda\pi_1 I_O^M + \lambda\pi_2 I_I^M + \lambda\pi_1 I_O^M + \lambda\pi_2 I_I^M$ and $\widetilde{\delta}N_L = \mu_L L_N + \mu_L L_R + \delta_N L_N + \delta_R L_R$.

Upon integration,

$$\lim_{\mathrm{t}\longrightarrow\infty} N_L(t) \leq \frac{\widetilde{\lambda}}{\widetilde{\delta}} \text{thus as } t \longrightarrow \infty \text{we have } N_L(t) \leq \frac{\widetilde{\lambda}}{\widetilde{\delta}}. \tag{20}$$

It then follows that the solution to the model equations exists in the region defined by

$$\Omega = \Omega_M \chi \Omega_f = \left\{\left(S_O^M, I_O^M, S_I^M, I_I^M, L_{R,} L_N\right)\varepsilon R_6^+\right\}. \tag{21}$$

Such that $S_O^M \geq 0, I_O^M \geq 0, S_I^M \geq 0, I_I^M \geq 0, L_R \geq 0, L_N \geq 0$.

$$\begin{gathered}\text{With } \Omega_M = \left(S_O^M + I_O^M + S_I^M + I_I^M\right) \leq \frac{\widetilde{\rho}}{\widetilde{\pi}}, \\ \Omega_f = \left(L_R + L_N\right) \leq \frac{\widetilde{\lambda}}{\widetilde{\delta}}.\end{gathered} \tag{22}$$

This proves the boundedness of the solution inside Ω which means that all the solutions to the model equations (2)–(7) starts and stays in Ω for all time $t \geq 0$. Generally, the solution to the initial value problems defined in Ω exists and is unique in the given interval. They remain bounded in the positively invariant and bounded region Ω; hence, the system is biologically and ecoepidemiologically well-posed, and the dynamics of the model can be sufficiently studied in Ω. □

3.3. Equilibrium Point Analysis. All systems of nonlinear differential equations may have none, one, many, or even infinite steady states [34]. In this study, we discuss the disease/larvae-free equilibrium points (E_0), insecticidal/control-free equilibrium points (E_C), and disease endemic equilibrium points (E_*).

3.3.1. Disease/Larvae-Free Equilibrium Points (E_0). The value of E_0 is obtained by setting all the infectious classes to zero, $\{L_N, L_R, I_O^M, I_I^M = 0\}$, with $\beta_0, \beta_1 = 0$ and $(S_O^{M'}, I_O^{M'}, S_I^{M'}, I_I^{M'}, L_R', L_N' = 0)$ to get

$$\begin{gathered}S_O^{M0} = \frac{\rho}{(1-\theta_1)\pi}, \\ I_I^{M0} = 0, \\ S_I^{M0} = \frac{\rho}{(1-\theta_2)\pi}, \\ I_I^{M0} = 0, \\ L_N^0 = 0, \\ L_R^0 = 0.\end{gathered} \tag{23}$$

3.3.2. Insecticidal/Control-Free Equilibrium Point (E_C). Let $E_C = (S_O^{Mc}, I_O^{Mc}, S_I^{Mc}, I_I^{Mc}, L_N^c, \text{and } L_R^c)$ denote the control-free equilibrium points. We solve the control equilibrium points by expressing it in terms of the force of infection β_0^c evaluated at the control-free equilibrium point. We set $(S_I^M, I_I^M = 0)$, $\{L_N, L_R, S_O^M, I_O^M \neq 0\}$, $(S_O^{M'}, I_O^{M'}, S_I^{M'}, I_I^{M'}, L_R', L_N' = 0), \delta_N = 0$, and $\delta_R = 0$ to get

$$
\begin{aligned}
S_O^{Mc} &= \frac{\rho}{(\beta_0^c + (1-\theta_1)\pi)},\\
I_O^{Mc} &= \frac{\beta_0^c}{\theta_1\pi}\left(\frac{\rho}{(\beta_0^c + (1-\theta_1)\pi)}\right),\\
S_I^{Mc} &= 0,\\
I_I^{Mc} &= 0,\\
L_N^c &= \frac{\rho(\beta_0^c\lambda\pi_1 + e_N\pi\lambda\theta_1)}{\pi\psi(\beta_0^c + \pi(1-\theta_1))\theta_1},\\
L_R^c &= \frac{(1-e_N)\lambda}{\mu_L} + \frac{\beta_0^c\lambda\rho\pi_1}{\pi\mu_L(\beta_0^c + \pi(1-\theta_1))\theta_1} + \frac{\rho\omega(\beta_0^c\lambda\pi_1 + e_N\pi\lambda\theta_1)}{\pi\mu_L\psi(\beta_0^c + \pi(1-\theta_1))\theta_1}.
\end{aligned}
\tag{24}
$$

We evaluated for the value of β_0^c, as $\beta_0^c = 1/2(b_1 + \sqrt{4b_0 + b_1^2})$. We let $\varpi = (\omega + \mu_L + \delta_N)$, $\sigma = (\mu_L + \delta_R)$, and $\psi = (\omega + \mu_L)$. Where $b_1 = \eta_O\lambda(\rho(\mu_L + \varepsilon(\psi + \omega)\pi_1) + \pi^2\ \theta_1\ \varepsilon\psi + e_N\varepsilon\psi - \rho\mu_N\psi\pi\theta_1)/(\rho\mu_N\psi)$, and $b_0 = \eta_O\lambda(\pi\theta_1\varepsilon\psi + e_N\pi\varepsilon\psi + e_N\rho(\mu_L + \varepsilon\omega + (-1 + e_N)b))/(\rho\mu_N\psi)$.

3.3.3. Disease Endemic Equilibrium Point (E_*). An endemic equilibrium point is a state in the model system where the disease in the population approaches a constant [22]. Let $E_* = S_O^{M*}, I_O^{M*}, S_I^{M*}, I_I^{M*}, L_N^*, L_R^*$ denote the disease endemic equilibrium point.

Solving for the system of equations (2)–(7) in terms of the force of infections β_0^* and β_I^*,

$$
\begin{aligned}
S_O^{M*} &= \frac{\rho}{(\beta_O^* + (1-\theta_1)\pi)},\\
I_O^{M*} &= \frac{\beta_O^*}{\theta_1\pi}\left(\frac{\rho}{(\beta_O^* + (1-\theta_1)\pi)}\right),\\
S_I^{M*} &= \frac{\rho}{(\beta_I^* + (1-\theta_2)\pi)},\\
I_I^{M*} &= \frac{\beta_I^*}{\theta_2\pi}\left(\frac{\rho}{\beta_I^* + (1-\theta_2)\pi}\right),\\
L_N^* &= \frac{\lambda}{\varpi}\left(e_N + \frac{\beta_o^*\rho\pi_1}{\pi(\beta_o^* + \pi(1-\theta_1))\theta_1} + \frac{\beta_I^*\rho\pi_2}{\pi(\beta_I^* + \pi(1-\theta_2))\theta_2}\right),\\
L_R^* &= \frac{\lambda}{\sigma}\left(1 - e_N + e_N\frac{\lambda\omega}{\varpi} + \frac{\rho(\varpi + \lambda\omega)\pi_1\beta_o^*}{\pi\varpi\theta_1(\pi + \beta_o^* - \pi\theta_1)} + \frac{\rho(\varpi + \lambda\omega)\pi_2\beta_I^*}{\pi\varpi\theta_2(\pi + \beta_I^* - \pi\theta_2)}\right).
\end{aligned}
\tag{25}
$$

Now, substituting the values of $S_O^{M*}, I_O^{M*}, S_I^{M*}, I_I^{M*}, L_N^*, L_R^*$ in β_0^* and β_I^* and introducing the relation $\eta_1\beta_0^* = \eta_0\beta_1^*$ which implies $\beta_1^* = \eta_1/\eta_0\beta_0^*$, $\beta_0^* = \eta_0/\eta_1\beta_1^*$ and then replacing into the values of the endemic equilibrium points to obtain the value of β_1^*.

For the model system to lie in the positively invariant region, we let the value of

$$
\begin{aligned}
\beta_1^* = -\frac{n_2}{3} &+ \frac{2^{1/3}\left(-3n_1 + n_2^2\right)}{3\left(-27n_0 + 9n_1n_2 - 2n_2^3 + \sqrt{4\left(3n_1 - n_2^2\right)^3 + \left(27n_0 - 9n_1n_2 + 2n_2^3\right)^2}\right)^{1/3}}\\
&+ \frac{\left(-27n_0 + 9n_1n_2 - 2n_2^3 + \sqrt{4\left(3n_1 - n_2^2\right)^3 + \left(27n_0 - 9n_1n_2 + 2n_2^3\right)^2}\right)^{1/3}}{32^{1/3.}}.
\end{aligned}
\tag{26}
$$

$\beta_1^* > 0$ if and only if $n_0, n_1, n_2 > 0$.

3.4. Basic Reproduction Number (R_0). R_0 is used to estimate the number of secondary infections that could arise if one infectious individual is introduced into a completely susceptible population [35]. We determine the value of R_0 using the next-generation matrix as discussed in [17]. We evaluate the Jacobian matrix of the model system of equations at DFEP and determine the spectral radius using Wolfram Mathematica software:

$$\text{DFEP}, \left\{E_0 = \left(S_O^{M0}, I_O^{M0}, S_I^{M0}, I_I^{M0}, L_N^0, L_R^0\right) = \left(\frac{\rho}{(1-\theta_1)\pi}, 0, \frac{\rho}{(1-\theta_2)\pi}, 0, 0, 0\right)\right\}. \tag{27}$$

The vector for the infected and infectious classes is denoted as $X = [I_O^M\ I_I^M\ L_N\ L_R]$, and the vector for the uninfected classes is denoted as $Y = [S_O^M S_I^M]$.

Using the notation f to denote the matrix for new infection and v to denote the matrix of the transfer of infections in the system,

$$f = \begin{pmatrix} \beta_O S_O^M \\ \beta_I S_I^M \\ 0 \\ 0 \end{pmatrix},$$

$$v = \begin{pmatrix} \theta_I \pi I_O^M \\ \theta_2 \pi I_I^M \\ -\lambda\left(e_N + \pi_1 I_O^M + \pi_2 I_I^M\right) + (\varpi) L_N, \\ -\left((1-e_N) + \pi_1 I_O^M + \pi_2 I_I^M\right)\lambda - \omega L_N + (\mu_L + \delta_R) L_R. \end{pmatrix}. \tag{28}$$

Evaluating the Jacobian matrices of f and v at DFEP to get $F = [\partial f/\partial X]_{E_0}$, $V = [\partial v/\partial X]_{E_0}$, and E_0 as the disease-free equilibrium point,

$$J(f)_{E_0} = F = \begin{pmatrix} \frac{\partial(\beta_O S_O^M)}{\partial I_O^M} & \frac{\partial(\beta_O S_O^M)}{\partial I_I^M} & \frac{\partial(\beta_O S_O^M)}{\partial L_N} & \frac{\partial(\beta_O S_O^M)}{\partial L_R} \\ \frac{\partial(\beta_O S_O^M)}{\partial I_O^M} & \frac{\partial(\beta_O S_O^M)}{\partial I_I^M} & \frac{\partial(\beta_I S_I^M)}{\partial L_N} & \frac{\partial(\beta_I S_I^M)}{\partial L_R} \\ 0 & 0 & 0 & 0 \\ 0 & 0 & 0 & 0 \end{pmatrix}_{E_O}, \tag{29}$$

with $\beta_O = \eta_O(L_N + \varepsilon L_R/N_M)$ and $\beta_I = \eta_I(L_N + \varepsilon L_R/N_M)$.

$$F = \begin{pmatrix} 0 & 0 & \left(\frac{\eta_O}{S_O^{M0}+S_I^{M0}}\right)S_O^{M0} & \left(\frac{\varepsilon\eta_O}{S_O^{M0}+S_I^{M0}}\right)S_I^{M0} \\ 0 & 0 & \left(\frac{\eta_I}{S_O^{M0}+S_I^{M0}}\right)S_I^{M0} & \left(\frac{\varepsilon\eta_I}{S_O^{M0}+S_I^{M0}}\right)S_I^{M0} \\ 0 & 0 & 0 & 0 \\ 0 & 0 & 0 & 0 \end{pmatrix} = \begin{pmatrix} 0 & 0 & \tilde{\eta}_O & \varepsilon\tilde{\eta}_O \\ 0 & 0 & \tilde{\eta}_I & \varepsilon\tilde{\eta}_I \\ 0 & 0 & 0 & 0 \\ 0 & 0 & 0 & 0 \end{pmatrix}. \tag{30}$$

Given that S_O^{M0}, S_I^{M0} and S_O^M, S_I^M were previously described as disease-free equilibrium points and their expression given in equation (23).

We let $\tilde{\eta}_o = (\eta_0(-1+\theta_2))/(-2+\theta_1+\theta_2)$, $\tilde{\eta}_1 = (\eta_1(-1+\theta_1))/(-2+\theta_1+\theta_2)$, $\varpi = (\omega+\mu_L+\delta_N)$, and $\sigma = (\mu_L+\delta_R)$.

$$J(v)_{E_0} = V = \begin{pmatrix} \theta_I\pi & 0 & 0 & 0 \\ 0 & \theta_2\pi & 0 & 0 \\ -\lambda\pi_I & -\lambda\pi_2 & (\varpi) & 0 \\ -\lambda\pi_I & -\lambda\pi_2 & -\omega & (\sigma) \end{pmatrix}, \tag{31}$$

$$V^{-1} = \begin{pmatrix} \frac{1}{\theta_I\pi} & 0 & 0 & 0 \\ 0 & \frac{1}{\theta_2\pi} & 0 & 0 \\ \frac{\lambda\pi_I}{\varpi\pi\theta_I} & \frac{\lambda\pi_2}{\varpi\pi\theta_2} & \frac{1}{\varpi} & 0 \\ \frac{\lambda\omega\pi_I+\lambda\pi_I\varpi}{\varpi\pi\sigma\theta_I} & \frac{\omega\lambda\pi_2+\lambda\pi_2\varpi}{\pi\varpi\sigma\theta_2} & \frac{\omega}{\varpi\sigma} & \frac{1}{\sigma} \end{pmatrix}. \tag{32}$$

The dominant eigenvalue in $G = \mathrm{FV}^{-1}$ is the value of $R_0 = \rho(\mathrm{FV}^{-1}) = \rho G$. It is the spectral radius of matrix G:

$$\mathrm{FV}^{-1} = \begin{pmatrix} \frac{(\lambda\varpi\pi_I+\lambda\pi_I\omega)\varepsilon\tilde{\eta}_O}{\pi\sigma\varpi\theta_I}+\frac{\lambda\pi_I\tilde{\eta}_O}{\pi\varpi\theta_I} & \frac{(\lambda\varpi\pi_2+\lambda\pi_2\omega)\varepsilon\tilde{\eta}_O}{\pi\sigma\varpi\theta_2}+\frac{\lambda\pi_2\tilde{\eta}_O}{\pi\varpi\theta_2} & \frac{\omega\varepsilon\tilde{\eta}_O}{\sigma\varpi}+\frac{\tilde{\eta}_O}{\omega} & \frac{\varepsilon\tilde{\eta}_O}{\sigma} \\ \frac{(\lambda\varpi\pi_I+\lambda\pi_I\omega)\varepsilon\tilde{\eta}_1}{\pi\sigma\varpi\theta_I}+\frac{\lambda\pi_I\tilde{\eta}_I}{\pi\varpi\theta_I} & \frac{(\lambda\varpi\pi_2+\lambda\pi_2\omega)\varepsilon\tilde{\eta}_I}{\pi\sigma\varpi\theta_2}+\frac{\lambda\pi_2\tilde{\eta}_I}{\pi\varpi\theta_2} & \frac{\omega\varepsilon\tilde{\eta}_1}{\sigma\varpi}+\frac{\tilde{\eta}_1}{\omega} & \frac{\varepsilon\tilde{\eta}_I}{\sigma} \\ 0 & 0 & 0 & 0 \\ 0 & 0 & 0 & 0 \end{pmatrix}. \tag{33}$$

The eigenvalues of the next-generation matrix G are determined using Wolfram Mathematica as

$$\left\{0, 0, 0, \frac{\lambda(\varpi\pi_2\varepsilon\tilde{\eta}_I\theta_I+\omega\pi_2\varepsilon\tilde{\eta}_I\theta_I+\sigma\pi_2\tilde{\eta}_I\theta_I+\varpi\pi_I\varepsilon\tilde{\eta}_O\theta_2+\omega\pi_I\varepsilon\tilde{\eta}_O\theta_2+\sigma\pi_I\tilde{\eta}_O\theta_2)}{\varpi\pi\theta_I\theta_2}\right\}. \tag{34}$$

Hence, the value of R_0 is

$$R_0 = \left\{ \frac{\lambda \pi_2 \tilde{\eta}_I}{\pi \varpi \theta_2} + \frac{\varepsilon \lambda \pi_2 \tilde{\eta}_I}{\pi \sigma \theta_2} + \frac{\varepsilon \lambda \omega \pi_2 \tilde{\eta}_I}{\pi \varpi \sigma \theta_2} + \frac{\lambda \pi_1 \tilde{\eta}_0}{\pi \varpi \theta_1} + \frac{\varepsilon \lambda \pi_1 \tilde{\eta}_0}{\pi \sigma \theta_1} + \frac{\varepsilon \lambda \omega \pi_1 \tilde{\eta}_0}{\pi \varpi \sigma \theta_1} \right\}. \tag{35}$$

3.4.1. Biological Interpretation of R_0. As shown in studies [17, 36], R_0 is defined as the expected number of secondary infections generated from a single primary infection in a completely susceptible population. In our model, the interactions present are organic maize-normal larvae interaction, organic maize-resistant larvae interaction, insecticidal sprayed maize-normal larvae interaction, and insecticidal sprayed maize-resistant larvae interaction. The basic reproduction number is consequently calculated as the sum of these interactions as follows:

$$R_0 = R_0^1 + R_0^2 + R_0^3 + R_0^4 + R_0^5 + R_0^6, \tag{36}$$

where $R_0^{\mathrm{In}} = R_0^1 + R_0^2 + R_0^3$ and $R_0^{\mathrm{Or}} = R_0^4 + R_0^5 + R_0^6$.

With $R_0^1 = (\lambda \pi_2 \tilde{\eta}_I / \pi \varpi \theta_2)$, $R_0^2 = (\varepsilon \lambda \pi_2 \tilde{\eta}_I / \pi \sigma \theta_2)$, and $R_0^3 = (\varepsilon \lambda \omega \pi_2 \tilde{\eta}_I / \pi \varpi \sigma \theta_2)$,

$$\begin{aligned} R_0^4 &= \frac{\lambda \pi_1 \tilde{\eta}_0}{\pi \varpi \theta_1}, \\ R_0^5 &= \frac{\varepsilon \lambda \pi_1 \tilde{\eta}_0}{\pi \sigma \theta_1}, \\ R_0^6 &= \frac{\varepsilon \lambda \omega \pi_1 \tilde{\eta}_0}{\pi \varpi \sigma \theta_1}. \end{aligned} \tag{37}$$

R_0^{In} represents the number of new infections on the insecticidal maize population $N_O^M(t)$ arising from both the normal larvae L_N and the resistant larvae L_R:

$$R_0^{\mathrm{In}} = \frac{\lambda \pi_2 \tilde{\eta}_I}{\pi \varpi \theta_2} + \frac{\varepsilon \lambda \pi_2 \tilde{\eta}_I}{\pi \sigma \theta_2} + \frac{\varepsilon \lambda \omega \pi_2 \tilde{\eta}_I}{\pi \varpi \sigma \theta_2}. \tag{38}$$

R_0^{Or} represents the number of new infections on the organic maize population $N_0^M(t)$ arising from both the normal larvae L_N and the resistant larvae L_R:

$$R_0^{\mathrm{Or}} = \frac{\lambda \pi_1 \tilde{\eta}_0}{\pi \varpi \theta_1} + \frac{\varepsilon \lambda \pi_1 \tilde{\eta}_0}{\pi \sigma \theta_1} + \frac{\varepsilon \lambda \omega \pi_1 \tilde{\eta}_0}{\pi \varpi \sigma \theta_1}. \tag{39}$$

3.5. Stability of Equilibrium Points. In this study, we determined the global asymptotic stability of the three model steady states using Castillo–Chavez, the Perron eigenvector, and the Lyapunov methods. The steady states are locally asymptotically stable if all the eigenvalues of the Jacobian matrix (J) evaluated at each (E) have negative real parts. The equilibrium point is asymptotically unstable if at least one of the eigenvalues has a positive real part. This is the linearity stability analysis theorem.

Let the model system of equations be denoted in vector form as

$$\frac{\mathrm{df}}{\mathrm{d}t} = f(y). \tag{40}$$

$y = (S_O^M(t), I_O^M(t), S_I^M(t), I_I^M(t), L_N(t), L_R(t))$.

We then write $f(y)$ in matrix form as

$$f(y) = \begin{pmatrix} \rho - \beta_O S_O^M - (1-\theta_1)\pi S_O^M \\ \beta_O S_O^M - \theta_1 \pi I_O^M \\ \rho - (1-\theta_2)\pi S_I^M - \beta_I S_I^M \\ \beta_I S_I^M - \theta_2 \pi I_I^M \\ \lambda\left(e_N + \pi_1 I_O^M + \pi_2 I_I^M\right) - (\omega + \mu_L + \delta_N) L_N \\ \left((1-e_N) + \pi_1 I_O^M + \pi_2 I_I^M\right)\lambda + \omega L_N - (\mu_L + \delta_R) L_R \end{pmatrix}. \tag{41}$$

The matrix $f(y)$ is used to evaluate the Jacobian matrix for the model system and thus the stability analysis for the various model stationary points.

3.5.1. Local Stability Analysis of the Disease-Free Equilibrium Point (E_0)

Theorem 4. *The disease-free equilibrium points for the FAW larvae-maize interaction model described by equations (1)–(6) are locally asymptotically stable if the below conditions are satisfied:*

(1) $a_1, a_2, a_3, a_4, a_5 > 0$

(2) $a_1 a_2 - a_3 > 0$

(3) $a_3(a_1 a_2 - a_3) - a_1(a_1 a_4 - a_5) > 0$

(4) $a_3^2 a_4 - a_1^2 a_4^2 - a_1 a_5 a_2^2 > 0$

Otherwise, E_0 is unstable.

Proof. Evaluating the Jacobian matrix at DFEP (shown in equation (23)), we get

$$\left(J_f\right)_{E_O} = \begin{pmatrix} -(1-\theta_1)\pi & 0 & 0 & 0 & -\tilde{\eta}_O & -\varepsilon\tilde{\eta}_O \\ 0 & -\theta_1\pi & 0 & 0 & \tilde{\eta}_O & \varepsilon\tilde{\eta}_O \\ 0 & 0 & -(1-\theta_2)\pi & 0 & -\tilde{\eta}_I & -\varepsilon\tilde{\eta}_I \\ 0 & 0 & 0 & -\theta_2\pi & \tilde{\eta}_I & \varepsilon\tilde{\eta}_I \\ 0 & \lambda\pi_1 & 0 & \lambda\pi_2 & -\varpi & 0 \\ 0 & \lambda\pi_1 & 0 & \lambda\pi_2 & \omega & -\sigma \end{pmatrix}. \tag{42}$$

The first eigenvalue of the above Jacobian matrix is $\lambda_1 = -(1-\theta_1)\pi$ which is less than zero and hence stable. Applying the Routh–Hurwitz stability criterion as shown by [37], the roots to characteristic equation (43) below have negative real parts if the coefficients a_i are nonnegative and matrices $J > 0$ for $i = 1, 2, 3, 4, 5$:

$$J_{f_{E_{0*}}} = \begin{pmatrix} -\theta_1\pi - \lambda & 0 & 0 & \tilde{\eta}_O & \varepsilon\tilde{\eta}_O \\ 0 & -(1-\theta_2)\pi - \lambda & 0 & -\tilde{\eta}_I & -\varepsilon\tilde{\eta}_I \\ 0 & 0 & -\theta_2\pi - \lambda & \tilde{\eta}_I & \varepsilon\tilde{\eta}_I \\ \lambda\pi_1 & 0 & \lambda\pi_2 & -\varpi - \lambda & 0 \\ \lambda\pi_1 & 0 & \lambda\pi_2 & \omega & -\sigma - \lambda \end{pmatrix}. \tag{43}$$

Using Mathematica software, the characteristic polynomial of the above matrix is evaluated as

$$a_0\lambda^5 + a_1\lambda^4 + a_2\lambda^3 + a_3\lambda^2 + a_4\lambda + a_5 = 0, \tag{44}$$

where $\lambda_i = 1(1)5$ are the eigenvalues.

By the Routh–Hurwitz criterion for stability analysis, the model system is proved to be locally asymptotically stable at disease-free steady state if and only if $a_1, a_2, a_3, a_4, a_5 > 0$, $a_1 a_2 - a_3 > 0$, $a_3(a_1 a_2 - a_3) - a_1(a_1 a_4 - a_5) > 0$, and $a_3^2 a_4 - a_1^2 a_4^2 - a_1 a_5 a_2^2 > 0$ shown in Table 3. Given that all the eigenvalues have negative real parts, it implies that the disease-free equilibrium point is locally asymptotically stable. □

3.5.2. Global Stability Analysis of the Disease-Free Equilibrium Point (E_0). To prove the global stability of the DFE points, we use a matrix-theoritic method defined by [38] to construct a Lyapunov function L involving the Perron eigenvector. Let $f(x)$ and x be defined as

$$\begin{aligned} f(x) &= (F - V)x - F(x) + V(x), \\ \text{where } x &= \left(I_O^M, I_I^M, L_N, L_R\right). \end{aligned} \tag{45}$$

Also, let us define the value $x' = (F - V)x - f(x)$ with the values of F and V as defined previously in Section 3.2 in equations (30) and (31), respectively. $\omega^T \geq 0$ is defined as the perron eigenvector or the left eigenvector corresponding to the eigenvalue $\rho(V^{-1}F) = \rho(FV^{-1}) = R_0$.

Theorem 5. *Consider F, V, and f(x) as defined in equations (30), (31), and (45). If $f(x) \geq 0$ in $\Omega \in R_+^6$, the model system $F \geq 0$, $V^{(-1)} \geq 0$ and $R_0 \leq 1$, then the function $L = W^T V^{(-1)} x$ is a Lyapunov function for the model systems (2)–(7) in Ω.*

Proof. We start by getting the derivative of L along the solutions to model equations (1)–(6):

$$\begin{aligned} L' &= \omega^T V^{-1} x' = \omega^T V^{-1}(F - V)x - \omega^T V^{-1} f(x), \\ \text{since } x' &= (F - V)x - f(x) = \left(R_0 - 1\right)\omega^T V^{-1} f(x). \end{aligned} \tag{46}$$

As shown above, since we have that $\omega^T \geq 0, V^{-1} \geq 0$ and $f(x) \geq 0$ in $\Omega \epsilon R_+^6$, then the last term is negative. If $R_0 \leq 1$, then $L' \leq 1$ in Ω, and thus, L is taken to be the Lyapunov function for the model system.

We determine

Table 3: Routh–Hurwitz criterion.

λ^5	a_0	a_2	a_4
λ^4	a_1	a_3	a_5
λ^3	$(a_4a_3 - a_5a_2)/a_4$	$(a_4a_1 - a_5a_0)/a_4$	0
λ^2	$(a_1a_2a_3 - a_3^2 - a_1^2a_4 - a_1a_5)/a_1a_2 - a_3$	$(a_5a_1a_2 - a_5a_3)/(a_2a_1 - a_3)$	0
λ^1	$(a_1a_2(a_3a_4 - a_2a_5) + a_5^2 + a_2a_3a_5 - (a_1^2a_4 - a_3^2)a_4)/(a_1a_2 - a_3)$	0	0
λ^0	0	0	0

$$\omega^T = \begin{bmatrix} \omega_1 & \omega_2 & \omega_3 & \omega_4 \end{bmatrix}^T = \omega^T V^{-1} F = R_0 \omega^T = \begin{bmatrix} 0 & 0 & 0 & 1 \end{bmatrix}^T. \tag{47}$$

Therefore,

$$V^{-1} = \begin{pmatrix} \dfrac{1}{\theta_I \pi} & 0 & 0 & 0 \\ 0 & \dfrac{1}{\theta_2 \pi} & 0 & 0 \\ \dfrac{\lambda \pi_I}{\varpi \pi \theta_I} & \dfrac{\lambda \pi_2}{\varpi \pi \theta_2} & \dfrac{1}{\varpi} & 0 \\ \dfrac{\lambda \omega \pi_I + \lambda \pi_I \varpi}{\varpi \pi \sigma \theta_I} & \dfrac{\omega \lambda \pi_2 + \lambda \pi_2 \varpi}{\varpi \sigma \pi \theta_2} & \dfrac{\omega}{\varpi \sigma} & \dfrac{1}{\sigma} \end{pmatrix}, \tag{48}$$

as generated in Section 3.2.

$$\omega^T V^{-1} = \begin{bmatrix} \dfrac{\lambda \omega \pi_I + \lambda \pi_I \varpi}{\varpi \pi \sigma \theta_I} \\ \dfrac{\omega \lambda \pi_2 + \lambda \pi_2 \varpi}{\varpi \sigma \pi \theta_2} \\ \dfrac{\omega}{\varpi \sigma} \\ \dfrac{1}{\sigma} \end{bmatrix}. \tag{49}$$

Thus,

$$L = \omega^T V^{-1} x = \left(\frac{\lambda \omega \pi_I + \lambda \pi_I \varpi}{\varpi \pi \sigma \theta_I} \right) I_0^M + \left[\frac{\omega \lambda \pi_2 + \lambda \pi_2 \varpi}{\varpi \sigma \pi \theta_2} \right] I_I^M + \left[\frac{\omega}{\varpi \sigma} \right] L_N + \left[\frac{1}{\sigma} \right] L_R. \tag{50}$$

Equation (50) becomes the Lyapunov function for the model system shown by equations (1)–(6).

By Perron–Frobenius, we let

$$V^{-1} F, \quad f(x) \geq 0. \tag{51}$$

With

$$f(x_0) = 0, \quad F \geq 0, \quad V^{-1} \geq 0, \tag{52}$$

to be irreducible and positive in $\Omega \epsilon R_+^6$, it follows then that $\omega^T > 0$. Hence, by LaSalle's invariant principle [39], $L' = 0$ shows that $\omega^T x = 0$ and $x = 0$.

Thus, our disease-free equilibrium point (E_0) is globally asymptotically stable.

We also prove that the disease-free equilibrium point is globally asymptotically stable using the Castillo–Chavez method as shown below.

We apply the method established by [40]. We start first by rewriting the system of model equations in the form:

$$\frac{dX}{dt} = F(X, Z), \quad \frac{dZ}{dt} = G(X, Z), \quad G(X, 0 = 0). \tag{53}$$

With $X = (S_0^M, S_I^M) \in R_+^2$ representing the uninfected classes and $Z = (I_0^M, I_I^M, L_N, \text{and } L_R) \in R_+^4$ representing the infected and the infectious classes, $E_0 = (X^*, 0)$ denotes the disease-free equilibrium point of the system $E_0 = \{(S_O^{M0}, I_O^{M0}, S_I^{M0}, I_I^{M0}, L_N^0, L_R^0) = (\rho/(1-\theta_1)\pi, 0, \rho/(1-\theta_2)\pi, 0, 0, 0)\}$.

According to the Castillo–Chavez stability theorem if the following conditions are satisfied in the points given above, then the global asymptotic stability of E_0 is guaranteed. The conditions include

$$1. \frac{dX}{dt} = F(X, 0). \tag{54}$$

X^* is globally asymptotically stable

$$2. \frac{dZ}{dt} = D_Z G(X, 0) Z - \widetilde{G}(X, Z), \widetilde{G}(X, Z) \geq 0, \quad \forall (X, Z) \in \Omega \in R_+^6. \tag{55}$$

□

Theorem 6. *The disease-free equilibrium point (E_0) is globally asymptotically stable.*

Proof. We start by dividing the model into subsystems:

$$X = \left(S_0^M, S_I^M\right),$$
$$Z = \left(I_0^M, I_I^M, L_N, L_R\right). \tag{56}$$

We then generate two vector-valued functions:

$$F(X,Z) = \begin{pmatrix} \rho - \beta_O S_O^M - (1-\theta_1)\pi S_O^M \\ \rho - (1-\theta_2)\pi S_I^M - \beta_I S_I^M \end{pmatrix},$$
$$G(X,Z) = \begin{pmatrix} \beta_O S_O^M - \theta_1 \pi I_O^M \\ \beta_I S_I^M - \theta_2 \pi I_I^M \\ \lambda\left(\pi_1 I_O^M + \pi_2 I_I^M\right) - (\omega + \mu_L + \delta_N)L_N \\ \left(\pi_1 I_O^M + \pi_2 I_I^M\right)\lambda + \omega L_N - (\mu_L + \delta_R)L_R \end{pmatrix}. \tag{57}$$

Evaluating for the reduced system from condition (1), $(\mathrm{dX}/\mathrm{d}t) = F(X,0)$ to get,

$$\frac{\mathrm{dS}_O^M}{\mathrm{d}t} = \rho - (1-\theta_1)\pi S_O^M,$$
$$\frac{\mathrm{dS}_I^M}{\mathrm{d}t} = \rho - (1-\theta_2)\pi S_I^M. \tag{58}$$

We note that the system has dynamics of an asymptomatic system independent of initial conditions in Ω.

We then compute $G(X,Z) = D_Z G(X^*,0)Z - \widetilde{G}(X,Z)$ and prove that $\widetilde{G}(X,Z) \geq 0$.

Let $A = D_Z G(X^*,0)$ be a Jacobian matrix of $\widetilde{G}(X,Z)$ taken in $Z = (I_0^M, I_I^M, L_N, L_R)$ and evaluated at $(X^*,0)$. It is also defined as an M matrix since all the nondiagonal elements are nonnegative:

$$A = \begin{pmatrix} \theta_1\pi & 0 & 0 & 0 \\ 0 & \theta_2\pi & 0 & 0 \\ \lambda\pi_1 & \lambda\pi_2 & -\varpi & 0 \\ \lambda\pi_1 & \lambda\pi_2 & \omega & -\sigma. \end{pmatrix}. \tag{59}$$

Evaluating the value of AZ,

$$AZ = \begin{pmatrix} \theta_1\pi I_0^M \\ \theta_2\pi I_I^M \\ \lambda\pi_1 I_0^M + \lambda\pi_2 I_I^M - \varpi L_N \\ \lambda\pi_1 I_0^M + \lambda\pi_2 I_I^M + \omega L_N - \sigma L_R \end{pmatrix}. \tag{60}$$

With the equation $\widetilde{G}(X,Z) = AZ - G(X,Z) \geq 0$, then the value of

$$\widetilde{G}(X,Z) = \begin{pmatrix} \beta_0 S_0^M \\ \beta_I S_I^M \\ 0 \\ 0 \end{pmatrix}. \tag{61}$$

Since $\widetilde{G}(X,Z) \geq 0 \quad \forall (X,Z) \in \Omega \in R_+^6$, then DFE is proved to be globally asymptotically stable. □

3.5.3. Local Stability Analysis of the Control-Free Equilibrium Point

Theorem 7. *The control-free equilibrium E_C point is locally asymptotically stable.*

Proof. The local stability analysis of the control-free steady state is achieved by first generating the Jacobian matrix $J_{f(E_C)=}$ evaluated at the control-free steady state evaluated in Section 3.3.2:

$$J_{f(E_C)=} \begin{pmatrix} -(1-\theta_1)\pi - a_0 & a_1 & a_1 & a_1 & a_2 & a_3 \\ a_0 & -a_1 - \theta_1\pi & -a_1 & a_1 & a_2 & a_3 \\ 0 & 0 & -(1-\theta_2)\pi - a_4 & 0 & 0 & 0 \\ 0 & 0 & a_5 & -\theta_2\pi & 0 & 0 \\ 0 & \lambda\pi_1 & 0 & \lambda\pi_2 & -\varpi & 0 \\ 0 & \lambda\pi_1 & 0 & \lambda\pi_2 & \omega & -\sigma \end{pmatrix}, \tag{62}$$

where $a_0 = ((L_N^c + \in L_R^c)\eta_0)/(S_O^{\mathrm{Mc}} + I_O^{\mathrm{Mc}}) - (S_O^{\mathrm{Mc}}(L_N^c + \in L_R^c)\eta_0/(S_O^{\mathrm{Mc}} + I_O^{\mathrm{Mc}})^2)$, $a_1 = (S_O^{\mathrm{Mc}}(L_N^c + \in L_R^c)\eta_0/(S_O^{\mathrm{Mc}} + I_O^{Mc})^2)$, $a_2 = (\eta_0 S_O^{\mathrm{Mc}})/(S_O^{\mathrm{Mc}} + I_O^{\mathrm{Mc}})$, $a_3 = (\epsilon\eta_0 S_O^{\mathrm{Mc}})/(S_O^{\mathrm{Mc}} + I_O^{\mathrm{Mc}})$, $a_4 = ((L_N^c + \in L_R^c)\eta_0)/(S_O^{\mathrm{Mc}} + I_O^{\mathrm{Mc}})$, and $a_5 = ((L_N^c + \in L_R^c)\eta_1)/(S_O^{\mathrm{Mc}} + I_O^{\mathrm{Mc}})$, with $L_N^C, L_R^C, S_O^{\mathrm{MC}}, I_O^{\mathrm{MC}}$ as shown in Section 3.3.2.

Using Wolfram Mathematica, the eigenvalues are found to be

$$\begin{aligned}
\gamma_1 = \gamma_2 = \gamma_3 = \gamma_{4=} &\left(\pi\varpi\sigma a_1\right)^4 + \big((\pi + \varpi + \sigma + a_0 + a_1) - \pi\lambda\sigma a_2\pi_1 - 2\lambda\sigma a_0 a_2\pi_1 - \pi\lambda\varpi a_3\pi_1 - \pi\lambda\omega a_3\pi_1 - 2\lambda\varpi a_0 a_3\pi_1 \\
&- 2\lambda\omega a_0 a_3\pi_1 + \pi^2\varpi\sigma\theta_1 + \pi\varpi\sigma a_0\theta_1 - \pi\varpi\sigma a_1\theta_1 + \pi\lambda\sigma a_2\pi_1\theta_1 + \pi\lambda\varpi a_3\pi_1\theta_1 + \pi\lambda\omega a_3\pi_1\theta_1 - \pi^2\varpi\sigma\theta_1^2\big)^3 \\
&+\big(\pi\varpi + \pi\sigma + \varpi\sigma + \varpi a_0 + \sigma a_0 + \pi a_1 + \varpi a_1 + \sigma a_1 - \lambda a_2\pi_1 - \lambda a_3\pi_1 + \pi^2\theta_1 + \pi a_0\theta_1 - \pi a_1\theta_1 - \pi^2\theta_1^2\big)^2 \\
&+\big(\pi\varpi\sigma + \varpi\sigma a_0 + \pi\varpi a_1 + \pi\sigma a_1 + \varpi\sigma a_1 - \pi\lambda a_2\pi_1 - \lambda\sigma a_2\pi_1 - 2\lambda a_0 a_2\pi_1 - \pi\lambda a_3\pi_1 - \lambda\varpi a_3\pi_1 - \lambda\omega a_3\pi_1 - 2\lambda a_0 a_3\pi_1 \\
&+ \pi^2\varpi\theta_1 + \pi^2\sigma\theta_1 + \pi\varpi a_0\theta_1 + \pi\sigma a_0\theta_1 - \pi\varpi a_1\theta_1 - \pi\sigma a_1\theta_1 + \pi\lambda a_2\pi_1\theta_1 + \pi\lambda a_3\pi_1\theta_1 - \pi^2\varpi\theta_1^2 - \pi^2\sigma\theta_1^2\big), \\
\gamma_5 = &-\pi\theta_2, \\
\gamma_6 = &-\pi - a_4 + \pi\theta_2.
\end{aligned} \tag{63}$$

Through back substitution, all the Eigen values are negative, and thus, the control-free equilibrium point is evaluated to be stable. □

3.5.4. Global Stability Analysis of the Control-Free Equilibrium Point (E_C). If a Lyapunov function to a linearized nonlinear system is obtained and exists, then it shows that the model system is asymptotically stable [41].

Theorem 8. *The control-free equilibrium point is globally asymptotically stable (i) if the insecticidal-free equilibrium is feasible and (ii) if the equilibrium point is a locally asymptotically stable solution.*

Proof. We consider a Lyapunov method for stability analysis, an approach adopted by [42]. We start by constructing a Lyapunov function:

$$L = \sum b_i\left(q_i - q_i^C \ln q_i\right). \tag{64}$$

b_i represents a constant selected such that $b_i > 0$, q_i represents the i^{th} compartments classes, and q_i^c represents the control-free equilibrium point of the i^{th} compartmental classes.

Expanding the Lyapunov function and substituting the compartments,

$$\begin{aligned}
L = b_1\left(S_0^M - S_0^{\mathrm{Mc}}\ln S_O^M\right) + b_2\left(I_0^M - I_0^{\mathrm{Mc}}\ln I_O^M\right) + b_3\left(S_I^M - S_I^{\mathrm{Mc}}\ln S_I^M\right) + b_4\left(I_I^M - I_I^{\mathrm{Mc}}\ln I_I^M\right) \\
+ b_5\left(L_N - L_N^c\ln L_N\right) + b_6\left(L_R - L_R^c\ln L_R\right).
\end{aligned} \tag{65}$$

We evaluate the derivative of equation (69) with respect to time to get

$$\frac{\mathrm{dL}}{\mathrm{d}t} = b_1\left(1 - \frac{S_0^{\mathrm{Mc}}}{S_O^M}\right)\frac{\mathrm{dS}_O^M}{dt} + b_2\left(1 - \frac{I_0^{\mathrm{Mc}}}{I_0^M}\right)\frac{\mathrm{dI}_0^M}{\mathrm{d}t} + b_3\left(1 - \frac{S_I^{\mathrm{Mc}}}{S_I^M}\right)\frac{\mathrm{dS}_I^M}{dt} + b_4\left(1 - \frac{I_I^{\mathrm{Mc}}}{I_I^M}\right)\frac{\mathrm{dI}_I^M}{\mathrm{d}t} + b_5\left(1 - \frac{L_N^c}{L_N}\right)\frac{\mathrm{dL}_N}{dt} + b_6\left(1 - \frac{L_R^c}{L_R}\right)\frac{\mathrm{dL}_R}{dt}, \tag{66}$$

where $S_0^M(t) = S_0^{\mathrm{Mc}}(t), I_0^M(t) = I_0^{\mathrm{Mc}}(t), S_I^M(t) = S_I^{\mathrm{Mc}}(t), I_I^M(t) = I_I^{\mathrm{Mc}}(t), L_N(t) = L_N^c(t), L_R(t) = L_R^c(t)$.

Substituting the values of (dS_O^M/dt), (dI_0^M/dt), (dS_I^M/dt), (dI_I^M/dt), (dL_N/dt), (dL_R/dt) with the model values, we get

$$\begin{aligned}\frac{dL}{dt} &= b_1\left(1-\frac{S_0^{Mc}}{S_O^M}\right)\left[\rho-\beta_O S_O^M-(1-\theta_1)\pi S_O^M\right]+b_2\left(1-\frac{I_0^{Mc}}{I_0^M}\right)\left[\beta_O S_O^M-\theta_1\pi I_O^M\right]\\ &+b_3\left(1-\frac{S_I^{Mc}}{S_I^M}\right)\left[\rho-(1-\theta_2)\pi S_I^M-\beta_I S_I^M\right]+b_4\left(1-\frac{I_I^{Mc}}{I_I^M}\right)\left[\beta_I S_I^M-\theta_2\pi I_I^M\right]\\ &+b_5\left(1-\frac{L_N^c}{L_N}\right)\left[\lambda\left(e_N+\pi_1 I_O^M+\pi_2 I_I^M\right)-(\omega+\mu_L+\delta_N)L_N\right]\\ &+b_6\left(1-\frac{L_R^c}{L_R}\right)\left[\left((1-e_N)+\pi_1 I_O^M+\pi_2 I_I^M\right)\lambda+\omega L_N-(\mu_L+\delta_R)L_R\right].\end{aligned} \tag{67}$$

As shown in Section 3.1, the model equations are positively invariant, and hence,

$$\frac{dL}{dt}\le 0 \quad \forall S_0^M(t), I_0^M(t), S_I^M(t), I_I^M(t), L_N(t), L_R(t)>0, \tag{68}$$

and also,

$$\frac{dL}{dt}=0 \text{ if } S_0^M(t)=S_0^{Mc}(t), I_0^M(t)=I_0^{Mc}(t), S_I^M(t)=S_I^{Mc}(t), I_I^M(t)=I_I^{Mc}(t), L_N(t)=L_N^c(t), L_R(t)=L_R^c(t). \tag{69}$$

It can be seen that the only invariant set in Ω where $dL/dt=0$ is the set $\{S_0^{Mc}(t), I_0^{Mc}(t), S_I^{Mc}(t), I_I^{Mc}(t), S_I^{Mc}(t), L_N^c(t), L_R^c(t) \in \Omega \in R_+^6\}$. Since $f(x)=0$ by LaSalle's invariance principle [39], (E_C) is globally asymptotically stable on Ω iff $R_0 \ge 0$. Otherwise, it is unstable. □

3.5.5. Global Stability Analysis of the Endemic Equilibrium Point E_*

Theorem 9. *For the endemic equilibrium point to be globally stable, (i) the endemic equilibrium point must be feasible and (ii) the endemic equilibrium point must be locally stable.*

Proof. We assume that the endemic equilibrium point is locally asymptotically stable since the linearization method evaluated at the equilibrium point proves to be mathematically complicated.

Applying the Lyapunov method as used by [42] and constructing the appropriate Lyapunov function, we get

$$L=\sum a_i\left(x_i-x_i^*\ln x_i\right), \tag{70}$$

where a_i represents a constant selected such that $b_i>0$, x_i represents the i^{th} compartments classes, and x_i^* represents the disease endemic equilibrium point (E_*) of the i^{th} compartment classes.

Expanding the Lyapunov function and substituting the compartments,

$$\begin{aligned}L &= a_1\left(S_0^M-S_0^{M*}\ln S_O^M\right)+a_2\left(I_0^M-I_0^{M*}\ln I_O^M\right)+a_3\left(S_I^M-S_I^{M*}\ln S_I^M\right)\\ &+a_4\left(I_I^M-I_I^{M*}\ln I_I^M\right)+a_5\left(L_N-L_N^*\ln L_N\right)+a_6\left(L_R-L_R^*\ln L_R\right).\end{aligned} \tag{71}$$

Differentiating equation (75) with respect to time, we get

$$\frac{dL}{dt} = a_1\left(1 - \frac{S_0^{M*}}{S_O^M}\right)\frac{dS_O^M}{dt} + a_2\left(1 - \frac{I_0^{M*}}{I_0^M}\right)\frac{dI_0^M}{dt} + a_3\left(1 - \frac{S_I^{M*}}{S_I^M}\right)\frac{dS_I^M}{dt} + a_4\left(1 - \frac{I_I^{M*}}{I_I^M}\right)\frac{dI_I^M}{dt} + a_5\left(1 - \frac{L_N^*}{L_N}\right)\frac{dL_N}{dt} + a_6\left(1 - \frac{L_R^*}{L_R}\right)\frac{dL_R}{dt}. \tag{72}$$

It is equivalent to

$$\begin{aligned}\frac{dL}{dt} = {} & a_1\left(1 - \frac{S_0^{M*}}{S_O^M}\right)\left[\rho - \beta_O S_O^M - (1-\theta_1)\pi S_O^M\right] + a_2\left(1 - \frac{I_0^{M*}}{I_0^M}\right)\left[\beta_O S_O^M - \theta_1 \pi I_O^M\right] + a_3\left(1 - \frac{S_I^{M*}}{S_I^M}\right)\left[\rho - (1-\theta_2)\pi S_I^M - \beta_I S_I^M\right] \\ & + a_4\left(1 - \frac{I_I^{M*}}{I_I^M}\right)\left[\beta_I S_I^M - \theta_2 \pi I_I^M\right] + a_5\left(1 - \frac{L_N^*}{L_N}\right)\left[\lambda\left(e_N + \pi_1 I_O^M + \pi_2 I_I^M\right) - (\omega + \mu_L + \delta_N)L_N\right] \\ & + a_6\left(1 - \frac{L_R^*}{L_R}\right)\left[\left((1-e_N) + \pi_1 I_O^M + \pi_2 I_I^M\right)\lambda + \omega L_N - (\mu_L + \delta_R)L_R\right],\end{aligned} \tag{73}$$

where $S_0^M(t) = S_0^{M*}(t), I_0^M(t) = I_0^{M*}(t), S_I^M(t) = S_I^{M*}(t), I_I^M(t) = I_I^{M*}(t), L_N(t) = L_N^*(t), L_R(t) = L_R^*(t)$.

As in Section 3.1, the model equations are positively invariant, and hence,

$$\begin{aligned}&\frac{dL}{dt} \le 0 \quad \forall S_0^M(t), I_0^M(t), S_I^M(t), I_I^M(t), L_N(t), L_R(t) > 0, \\ &\frac{dL}{dt} = 0 \text{ if } S_0^M(t) = S_0^{M*}(t), I_0^M(t) = I_0^{M*}(t), S_I^M(t) = S_I^{M*}(t), I_I^M(t) = I_I^{M*}(t), L_N(t) = L_N^*(t), L_R(t) = L_R^*(t).\end{aligned} \tag{74}$$

It can be seen that the largest invariant set in Ω where $dL/dt = 0$ is the set $\{S_0^{(M^*)}(t), I_0^{(M^*)}(t), S_I^{(M^*)}(t), I_I^{(M^*)}(t), S_I^{(M^*)}(t), L_N^*(t), L_R^*(t) \in \Omega \in R_+^6\}$. Since $f(x) = 0$ by LaSalle's invariance principle [39], E_* is globally asymptotically stable on Ω iff $R_0 \ge 0$. Otherwise it is unstable. □

3.6. Sensitivity Analysis of R_0. Sensitivity analysis of R_0 helps identify the key parameters that significantly affect the FAW larvae-maize interaction model. This helps determine the key parameters to consider in the control strategies against FAW larvae infestation in the maize population by managing the value of the basic reproduction number and the infection. We follow a sensitivity method as conducted by [17, 18].

Definition 10. The normalized forward sensitivity index of a variable R_0, depending differentially on parameter P, is defined by an equation:

$$\alpha_{P'}^{R_0} = \frac{\partial R_0}{\partial P'}.\frac{P'}{R_0}, \tag{75}$$

where R_0 represents the basic reproduction number and P' represents all the main parameters.

In our study, we have the value of R_0 given as

$$R_0 = \frac{\lambda(\varepsilon\varpi + \sigma + \varepsilon\omega)(\pi_2\theta_1\tilde{\eta}_I + \pi_1\theta_2\tilde{\eta}_0)}{\pi\varpi\sigma\theta_1\theta_2}. \tag{76}$$

The sensitivity index of R_0 to λ is

$$\begin{aligned}\alpha_\lambda^{R_0} &= \frac{\partial R_0}{\partial \lambda}.\frac{\lambda}{R_0} \\ &= \frac{(\varepsilon\varpi + \sigma + \varepsilon\omega)(\pi_2\theta_1\tilde{\eta}_I + \pi_1\theta_2\tilde{\eta}_0)}{\pi\varpi\sigma\theta_1\theta_2}.\frac{\lambda}{(\lambda(\varepsilon\varpi + \sigma + \varepsilon\omega)(\pi_2\theta_1\tilde{\eta}_I + \pi_1\theta_2\tilde{\eta}_0)/\pi\varpi\sigma\theta_1\theta_2)} = 1.\end{aligned} \tag{77}$$

Table 4: Sensitivity indices.

Parameter	Sensitivity index
λ	1
σ	−0.5
ϖ	−0.5
ε	0.5
ω	0.2
π	−0.5
π_1	0.5
π_2	0.4
θ_1	−0.5
θ_2	−0.4

Table 5: Parameter values, ranges, and references.

Parameter	Description	Parameter value	Source/reference
θ_1	The harvesting rate of organic maize population $N_O^M(t)$	0.015	[17]
K	Maximum plant carrying capacity of the two maize sections	1000 plants	[17]
θ_2	The harvesting rate of insecticidal sprayed maize population $N_I^M(t)$	0.005	Estimated
e_N	The natural recruitment rate of larvae from the naturally occurring FAW population	0.98	[12]
ω	The rate at which normal larvae progress into resistant larvae population	0.45	[19]
ρ	The natural recruitment rate of the maize biomass into the maize population	50 kg per plant	[19]
μ_L	Total population decrease rate of the larvae	0.077	Calculated
μ_2	Progression rate into the pupal FAW life cycle	0.071	[12]
μ_1	The natural death rate of the FAW larvae	0.0071	[12]
δ_R	The insecticidal-induced death rates on the resistant larvae	0.35	[43]
δ_N	The insecticidal-induced death rates in the normal larvae	0.52	[43]
η_0	Infection factor	0.3922	Estimated
η_1	Infection factor	0.1087	Estimated
β_0	The rate of infection in the organic maize population	0.0202	Calculated
β_1	The rate of infection in the insecticidal maize population	0.0056	Calculated
λ	The survival rate of the larvae from the egg stage of the FAW population	0.75	[19]
π	The lost maize biomass in the $N_M(t)$ class was due to a caterpillar attack	0.9	[43]
π_1	The maize biomass from the $I_O^M(t)$ class contributing directly to the larvae increased the natural recruitment rate	0.2	[43]
π_2	The maize biomass from the $I_I^M(t)$ class contributing directly to the larvae increased the natural recruitment rate	0.18	Estimated

A similar procedure is used to calculate the sensitivity indices for the other parameters around the basic reproduction number; the results are shown in the Table 4.

3.6.1. Interpreting the Sensitivity Indices. Sensitivity indices for the basic reproduction number R_0 presented in the table above show positive and negative values for the parameter values. A positive sensitivity index denotes a direct linkage between the parameter and the basic reproduction number, while a negative sensitivity index denotes an inverse linkage between the parameter and the basic reproduction number. From the table, $(\lambda, \varepsilon, \omega, \pi_1, \text{and } \pi_2)$ have positive sensitivity indices. This means that the parameter values have a great impact on spreading the disease among the maize population upon an increase in their parameter values. This is because the value of R_0 will tend to increase by increasing the parameter values, further increasing the number of secondary infections in the susceptible maize population.

The parameters $(\sigma, \varpi, \theta_1, \theta_2)$ have negative sensitivity indices. This means that the value of R_0 decreases when their values are increased. This results in a decrease in the rate of infection, lowering the secondary infections in the susceptible maize population. The value of λ being equal to 1 means a unit increase in λ results in a unit increase in the value of R_0 and vice versa.

4. Numerical Simulation

4.1. Parameter Estimation. Numerical analysis of the model is conducted using a MATLAB inbuilt solver based on the Runge–Kutta order of 5 with parameter values cited in Table 5 as obtained from published studies together with a few estimated values. The initial value states are used as $S_O^M(0) = 1000$, $I_O^M(0) = 0$, $S_I^M(0) = 1000$, $I_I^M(0) = 0, L_N(0) = 100$, $L_R(0) = 10$ as shown by similar studies on the fall armyworm-maize interaction [17, 19, 43]. The simulations are conducted at a time range of between 0 and 60 days which is the vegetative stage of the maize population and the most interactive phase with the FAW population. The resulting simulation graphs are presented in Figures 2–11.

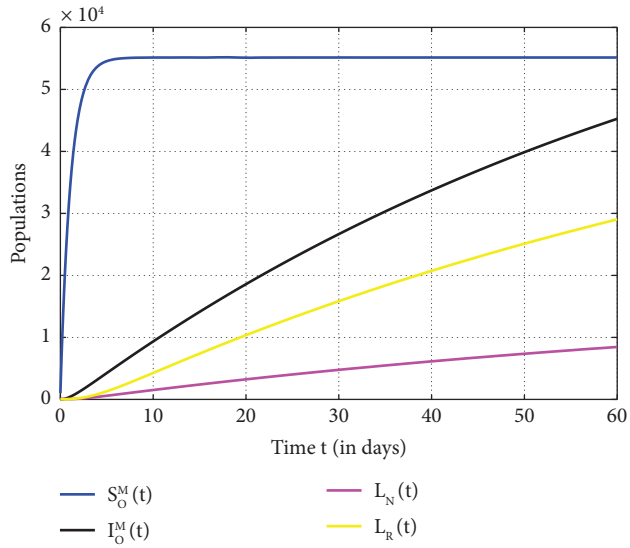

Figure 2: Population dynamics of organic maize interacting with the normal and resistant larvae.

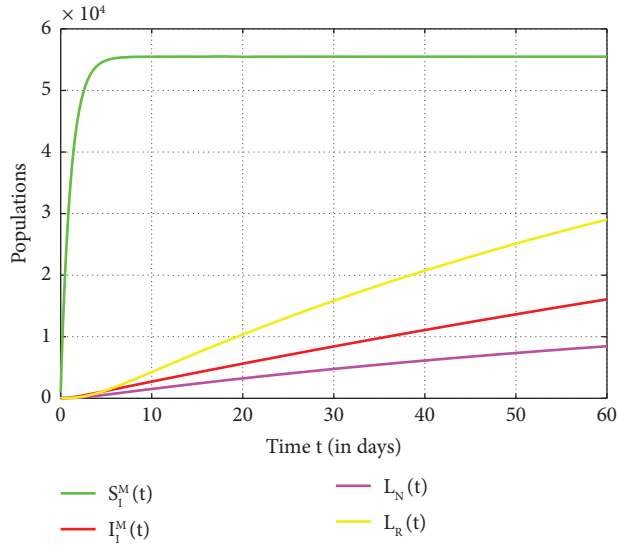

Figure 3: Population dynamics of insecticidal maize interacting with the normal and resistant larvae.

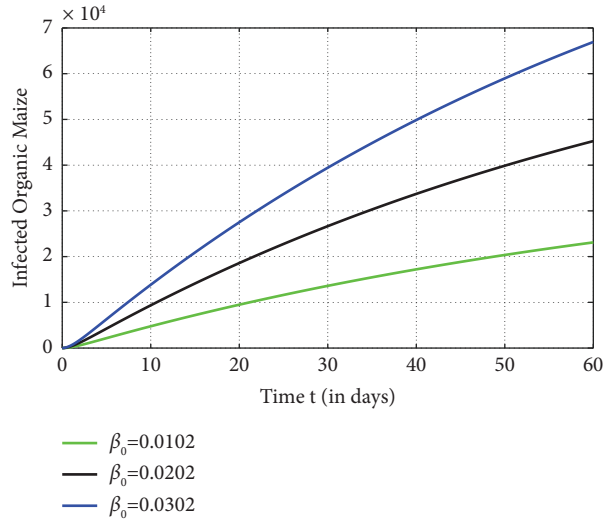

Figure 4: Population dynamics of infected organic maize at distinct values of β_0.

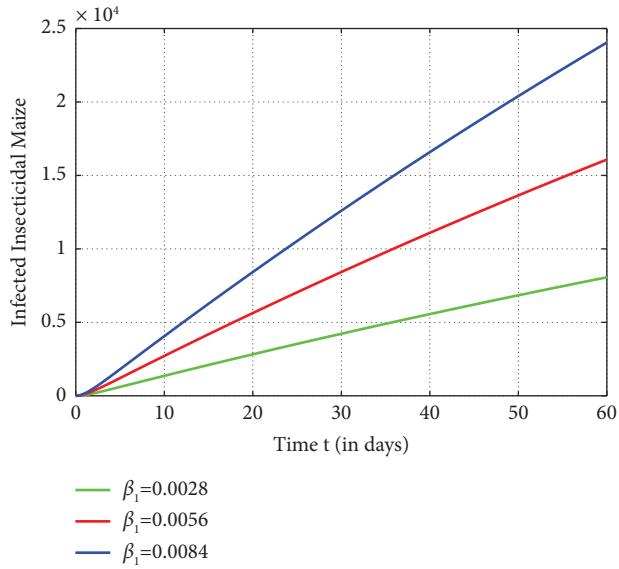

Figure 5: Population dynamics of infected insecticidal maize at distinct values of β_1.

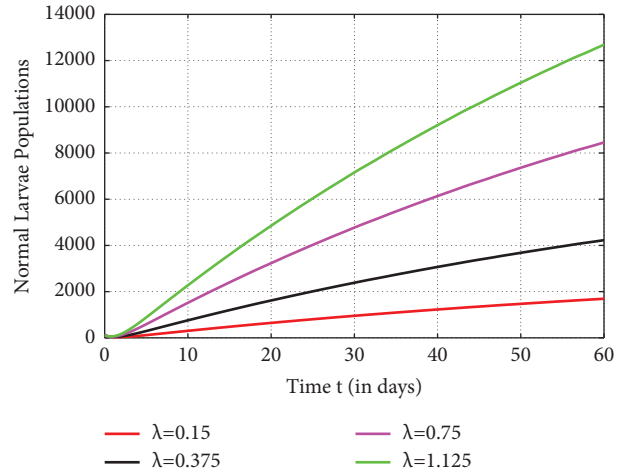

Figure 6: Population dynamics of normal larvae at distinct values of λ.

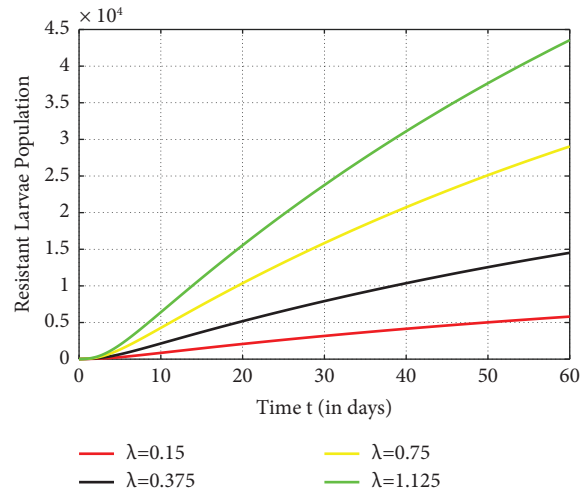

Figure 7: Population dynamics of resistant larvae at distinct values of λ.

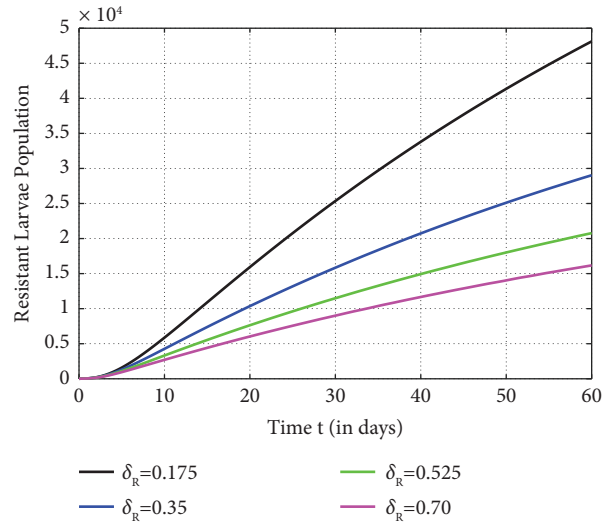

Figure 8: Population dynamics of resistant larvae at distinct values of δ_R.

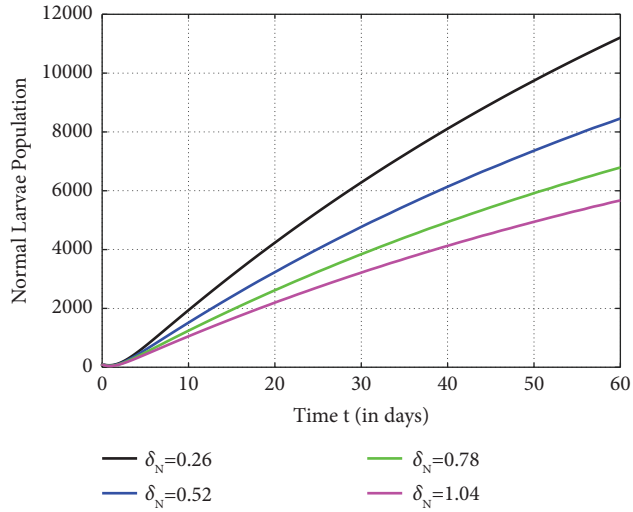

Figure 9: Population dynamics of normal larvae at distinct values of δ_N.

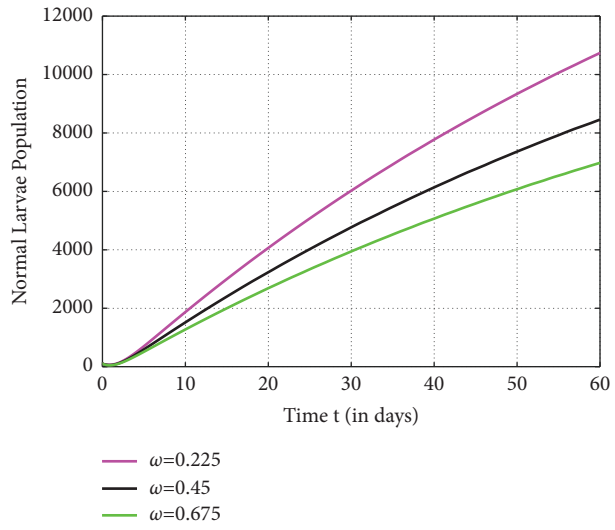

Figure 10: Population dynamics of normal larvae at distinct values of ω.

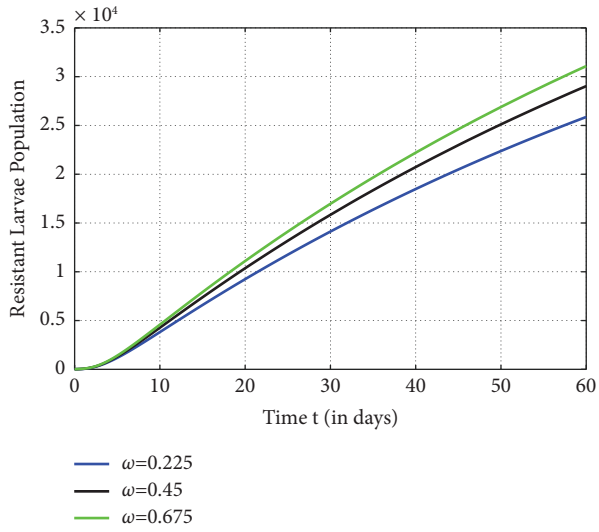

Figure 11: Population dynamics of resistance larvae at distinct values of ω.

4.2. Simulation Results. In Figures 2 and 3, the susceptible maize populations $\{S_O^M(t), S_I^M(t)\}$ increase exponentially with time until they reach the endemic equilibrium point. The curve for the organic infected maize in Figure 2 is observed to be higher than the curve for the infected insecticidal maize population in Figure 3. This is the effect of uncontrolled FAW larvae-organic maize interactions, which subsequently leads to a high force of infection (β_0) resulting in a higher infected organic maize population.

In Figure 4, when β_0 is decreased by 50%, the infected organic maize population decreases exponentially with time. This is due to the direct linkage between the force of infection and the basic reproduction number. At a higher value of β_0, the infected organic maize population increases exponentially. Similar observations are made in Figure 5; however, the infected insecticidal maize population occurs in lower rates as compared to the organic section. This is due to the lower values of β_1 as compared to β_0.

According to the model flowchart (Figure 1), λ represents the survival rate for the FAW larvae. From Figures 6 and 7, reducing the value of λ to lower values than the baseline value $\lambda = 0.75$ subsequently reduces the population of the normal and the resistant larvae. This has a direct effect on the force of infection in the maize population.

δ_R and δ_N denote the insecticidal-induced death rate on the resistant and normal larvae, respectively. In Figures 8 and 9, increasing the values of δ_R and δ_N reduces the population of the resistant and the normal larvae. This in turn reduces the infection rate leading to a lower basic reproduction number. We also observe that the resistant larvae are large in numbers as compared to normal larvae which pose a greater risk in the insecticide control measures.

From Figures 10 and 11, ω represents the rate at which the normal larvae progress into resistant larvae after contact with insecticidal sprays. At higher values of ω, more normal larvae, which are easy to eradicate from the model population by insecticides, progress into resistant larvae. This subsequently reduces the normal larvae population and increases the resistant larvae population.

5. Discussion and Conclusion

This study developed and analyzed a deterministic ecoepidemiological model on the maize-FAW interaction in the presence of insecticides and resistance factors. The model was proved to be uniformly bounded and positively invariant. Three equilibrium points, that is, the disease/larvae-free, control-free, and endemic equilibrium points, were established and evaluated to be locally and globally asymptotically stable at $R_0 \leq 1$. Furthermore, an expression for the basic reproduction number R_0 and its sensitivity analysis were conducted. The results showed that an increase in $\omega, \lambda, \beta_O, \beta_I$ and a decrease in δ_R, δ_N greatly increased the FAW population dynamics, increased the maize-FAW larvae interaction, and hence the spread of the disease to the susceptible maize population. Through numerical simulation, graphical results of the FAW-maize interaction and population dynamics are presented by applying parameter values obtained from literature and cited studies accordingly.

The analysis of R_0 in the host-pest (maize-FAW) interaction model helps determine how effective the insecticide control measures against the FAW larvae are and how to effectively use the control measures to reduce the value of R_0 to a value of less than one [13]. Increasing the forces of infection (β_0, β_1) increased the number of infected maize populations, while reducing the infection forces resulted in a decrease in the number of infected maize populations in both the organic and insecticidal sections. This was attributed to the direct impact of the force of infection on the basic reproduction number. The insecticide control measures used to control FAW-maize interactions in the insecticidal maize section ensured a reduced contact rate, and thus, the number of resulting secondary infections at

any time t was lower than in the organic uncontrolled FAW-maize interactions.

ω is a parameter value used in the model to represent a constant rate at which the normal larvae progress into resistant larvae after insecticide spraying. When insecticides are used to control the FAW larvae population, a few mutants in the population tolerate chemical insecticides better, while the normal population succumbs to them [44]. Resistance ω increased the infection rates by increasing the FAW larvae survival rate λ and reducing the insecticidal efficacy by lowering the larvae insecticidal-induced death rates δ_R and δ_N. However, while resistance affects both the organic and the insecticidal controlled maize sections, the FAW-maize interactions and thus the infection rates are lower in the controlled insecticidal sections than in the organic uncontrolled section.

Generally, the results from the model analysis showed that the FAW survival rate λ, resistance formation ω, and the insecticidal-induced death rates δ_R and δ_N are essential in controlling both the normal and the resistant FAW larvae. Control intervention aimed at reducing the infection rate in organic and insecticidal maize populations should aim at reducing these parameter factors. This is by using high-efficacy insecticides, resulting in higher FAW larvae death rates (δ_R, δ_N), thus reducing the FAW survival rate λ. The sensitivity analysis of R_0 showed that the FAW survival rate λ significantly affects the FAW-maize interactions. This informs both the organic and the inorganic farmers on the importance of using chemical control methods that are highly effective in reducing the FAW survival rate λ.

Various integrated FAW-maize management approaches should be adopted where several pest control methods are used together since no control method has been reported to work best in isolation. This will help reduce the high rate of resistance formation observed in FAW larvae, thus reducing their population dynamics. African countries should conduct proper civic education on pest control methods, FAW-maize interaction patterns, and resistance formation in insecticides used to ensure environmental conservation and minimize pest resistance formation. This is due to FAW's unique characteristics of high migration, mutation, and reproduction, which makes its control a bit expensive and difficult. However, the findings from this study are not exhaustive. In future studies, we will consider developing an optimal larvae survival control theory with resistance factors to achieve a profitable FAW larvae control strategy.

Data Availability

The research data used for the model analysis were obtained from previously published articles duly cited in this paper. Table 5 and other pertinent locations in this work provide references to the published articles.

Conflicts of Interest

The authors declare that they have no conflicts of interest.

Acknowledgments

The first author would like to thank the Board of Postgraduate Studies and the Department of Mathematics and Statistics at the University of Embu for their support to join the Master's program and continue in research work.

References

[1] R. Alvarenga, J. C. Moraes, A. M. Auad, M. Coelho, and A. M. Nascimento, "Induction of resistance of corn plants to Spodoptera frugiperda (J. E. Smith, 1797) (Lepidoptera: noctuidae) by application of silicon and gibberellic acid," *Bulletin of Entomological Research*, vol. 107, no. 4, pp. 527–533, 2017.

[2] K. Rosent rater and R. Suleiman, "Maize utilization in India: an overview," *American Journal of Food and Nutrition*, vol. 4, no. 6, pp. 169–176, 2016.

[3] H. G. Gebreziher, "Review on management methods of fall armyworm (Spodoptera frugiperda JE smith) in sub- saharan Africa," *International Journal of Entomology Research*, vol. 5, no. 2, pp. 09–14, 2020.

[4] J. K. Westbrook, R. N. Nagoshi, R. L. Meagher, S. J. Fleischer, and S. Jairam, "Modeling seasonal migration of fall armyworm moths," *International Journal of Biometeorology*, vol. 60, no. 2, pp. 255–267, 2016.

[5] M. L. Russo, L. R. Jaber, A. C. Scorsetti, F. Vianna, M. N. Cabello, and S. A. Pelizza, "Effect of entomopathogenic fungi introduced as corn endophytes on the development, reproduction, and food preference of the invasive fall armyworm Spodoptera frugiperda," *Journal of Pest Science*, vol. 94, no. 3, pp. 859–870, 2021.

[6] S. N. Gichere, K. S. Khakame, and O. Patrick, "Susceptibility evaluation of fall armyworm (Spodoptera frugiperda) infesting maize in Kenya against a range of insecticides," *Journal of Toxicology*, vol. 2022, Article ID 8007998, 11 pages, 2022.

[7] M. Y. Osae, J. O. Frimpong, J. O. Sintim, B. K. Offei, D. Marri, and S. E. K. Ofori, "Evaluation of different rates of ampligo insecticide against fall armyworm (spodoptera frugiperda (je smith);lepidoptera: noctuidae) in the coastal savannah agroecological zone of ghana," *Advances in Agriculture*, vol. 2022, Article ID 5059865, 14 pages, 2022.

[8] F. Assefa and D. Ayalew, "Status and control measures of fall armyworm (Spodoptera frugiperda) infestations in maize fields in Ethiopia: a review," *Cogent Food and Agriculture*, vol. 5, no. 1, Article ID 1641902, 2019.

[9] P. M. Matova, C. N. Kamutando, C. Magorokosho, D. Kutywayo, F. Gutsa, and M. Labuschagne, "Fall-armyworm invasion, control practices and resistance breeding in Sub-Saharan Africa," *Crop Science*, vol. 60, no. 6, pp. 2951–2970, 2020.

[10] C. B. Tanyi, R. N. Nkongho, J. N. Okolle, A. S. Tening, and C. Ngosong, "Effect of intercropping beans with maize and botanical extract on fall armyworm (Spodoptera frugiperda) infestation," *International Journal of Agronomy*, vol. 2020, Article ID 4618190, 7 pages, 2020.

[11] R. Day, P. Abrahams, M. Bateman et al., "Fall armyworm: impacts and implications for Africa," *Outlooks on Pest Management*, vol. 28, no. 5, pp. 196–201, 2017.

[12] H. De Groote, S. C. Kimenju, B. Munyua, S. Palmas, M. Kassie, and A. Bruce, "Spread and impact of fall armyworm (Spodoptera frugiperda J.E. Smith) in maize production areas of Kenya," *Agriculture, Ecosystems & Environment*, vol. 292, no. January, Article ID 106804, 2020.

[13] S. Daudi, L. Luboobi, M. Kgosimore, and D. Kuznetsov, "Dynamics for a non-autonomous fall armyworm-maize interaction model with a saturation functional response," *Mathematical Biosciences and Engineering*, vol. 19, no. 1, pp. 146–168, 2022.

[14] G.-S. Lee, "First report of the fall armyworm, Spodoptera frugiperda (smith, 1797) (Lepidoptera, noctuidae), a new migratory pest in korea," *Korean Journal of Applied Entomology*, vol. 59, no. 1, pp. 2287–2545, 2020.

[15] M. A. Lewis, S. V. Petrovskii, and J. R. Potts, *The Mathematics behind Biological Invasions*, vol. 44, Springer, Berlin, Germany, 2016.

[16] S. Chander and K. Arya, "Simulation of leaf folder, Cnaphalocrocis medinalis (Guenee), damage on rice for developing decision support tools," *International Journal of Pest Management*, vol. 62, no. 1, pp. 20–29, 2016.

[17] H. T. Alemneh, O. D. Makinde, and D. Mwangi Theuri, "Ecoepidemiological model and analysis of MSV disease transmission dynamics in maize plant," *International Journal of Mathematics and Mathematical Sciences*, vol. 2019, Article ID 7965232, 14 pages, 2019.

[18] A. G. Garcia, C. P. Ferreira, W. A. C. Godoy, and R. L. Meagher, "A computational model to predict the population dynamics of Spodoptera frugiperda," *Journal of Pest Science*, vol. 92, no. 2, pp. 429–441, 2019.

[19] S. Daudi, L. Luboobi, M. Kgosimore, and D. Kuznetsov, "Modelling the control of the impact of fall armyworm (Spodoptera frugiperda) infestations on maize production," *International Journal of Differential Equations*, vol. 2021, Article ID 8838089, 16 pages, 2021.

[20] J. O. Ochwach, M. O. Okongo, and M. M. Muraya, "Mathematical modeling of host- pest interac- tions in stage-structured populations: a case of false codling moth [thaumatotibia leucotreta]," *Journal of Progressive Research in Mathematics*, vol. 18, no. 4, pp. 1–21, 2021.

[21] A. Ben Dhahbi, Y. Chargui, S. M. Boulaaras, and S. Ben Khalifa, "A one-sided competition mathematical model for the sterile insect technique," *Complexity*, vol. 2020, no. Ci, Article ID 6246808, 12 pages, 2020.

[22] P. O. Affi, "Global stability analysis of the SEIR deterministic model in the presence of treatment at the latent period," *Applied Mathematics Letters*, vol. 4, no. 4, pp. 67–73, 2018.

[23] A. O. Victor and H. K. Oduwole, "Stability analysis of disease free equilibrium state (E0) for an endemic deterministic model for HIV/AIDS," *medRxiv*, 2020.

[24] J. Páez Chávez, D. Jungmann, and S. Siegmund, "Modeling and analysis of integrated pest control strategies via impulsive differential equations," *International Journal of Differential Equations*, vol. 2017, Article ID 1820607, 18 pages, 2017.

[25] A. K. Misra, R. Patel, and N. Jha, "Modeling the effects of insecticides and external efforts on crop production," *Nonlinear Analysis Modelling and Control*, vol. 26, no. 6, pp. 1012–1030, 2021.

[26] C. Wang, "A General Epidemic Model and Its Application to Mask Design Considering Different Preferences towards Masks," *Complexity*, vol. 2022, Article ID 1626008, 13 pages, 2022.

[27] K. R. Cheneke, K. P. Rao, and G. K. Edessa, "Fractional derivative and optimal control analysis of cholera epidemic model," *Journal of Mathematics*, vol. 2022, no. iii, Article ID 9075917, 17 pages, 2022.

[28] J. D. Sachs, "From millennium development goals to sustainable development goals," *The Lancet*, vol. 379, no. 9832, pp. 2206–2211, 2012.

[29] T. T. Ega and R. C. Ngeleja, "Mathematical model formulation and analysis for COVID-19 transmission with virus transfer media and quarantine on arrival," *Computational and Mathematical Methods*, vol. 2022, Article ID 2955885, 16 pages, 2022.

[30] Z. Iqbal, N. Ahmed, D. Baleanu et al., "Positivity and boundedness preserving numerical algorithm for the solution of fractional nonlinear epidemic model of HIV/AIDS transmission," *Chaos, Solitons and Fractals*, vol. 134, Article ID 109706, 2020.

[31] K. R. Cheneke, K. P. Rao, and G. K. Edesssa, "A new generalized fractional-order derivative and bifurcation analysis of cholera and human immunodeficiency Co-infection dynamic transmission," *International Journal of Mathematics and Mathematical Sciences*, vol. 2022, Article ID 7965145, 15 pages, 2022.

[32] A. Rodkina and H. Schurz, "On positivity and boundedness of solutions of nonlinear stochastic difference equations," *Discrete and Continuous Dynamical Systems*, vol. 2009, pp. 640–649, 2009.

[33] A. M. Society and M. Tables, "On the numerical solution of equations involving differential operators with constant coefficients," *American Mathematical Society*, vol. 6, no. 40, pp. 219–223, 2008.

[34] J. Harianto, "Local stability analysis of an SVIR epidemic model," *Cauchy*, vol. 5, no. 1, pp. 20–28, 2017.

[35] F. M. Guerra, S. Bolotin, G. Lim et al., "The basic reproduction number (R0) of measles: a systematic review," *The Lancet Infectious Diseases*, vol. 17, no. 12, pp. e420–e428, 2017.

[36] M. Ronoh, F. Chirove, S. A. Pedro et al., "Modelling the spread of schistosomiasis in humans with environmental transmission," *Applied Mathematical Modelling*, vol. 95, pp. 159–175, 2021.

[37] R. N. Clark, "The Routh-Hurwitz stability criterion, revisited," *IEEE Control Systems*, vol. 12, no. 3, pp. 119-120, 1992.

[38] P. Koutsourelakis, "Accurate uncertainty quantification using inaccurate computational models," *SIAM Journal on Scientific Computing*, vol. 31, no. 5, pp. 3274–3300, 2009.

[39] A. Arsie and C. Ebenbauer, "Refining lasalle's invariance principle," in *Proceedings of the 2009 American Control Conference*, pp. 108–112, St. Louis, MO, USA, July, 2009.

[40] C. Castillo-Chavez, Z. Feng, and W. Huang, "On the computation of RO and its role in global stability," *Institute for Mathematics and Its Applications*, vol. 1, pp. 125–229, 2002.

[41] S. A. Al-Sheikh, "Modeling and analysis of an SEIR epidemic model with a limited resource for treatment," *Global Journal of Science Frontier Research*, vol. 12, 14 pages, 2012.

[42] P. K. Maini and A. Korobeinikov, "A Lyapunov function and global properties for SIR and SEIR epidemiological models with nonlinear incidence," *Mathematical Biosciences and Engineering*, vol. 1, no. 1, pp. 57–60, 2004.

[43] W. B. Jamieson, "DigitalCommons @ university of Nebraska-lincoln individual based model to simulate the evolution of insecticide resistance," Department of Mathematics: Dissertations, Theses, and Student Research, 2019.

[44] K. Charaabi, S. Boukhris-Bouhachem, M. Makni, and I. Denholm, "Occurrence of target-site resistance to neonicotinoids in the aphid *Myzus persicae* in Tunisia, and its status on different host plants," *Pest Management Science*, vol. 74, no. 6, pp. 1297–1301, 2018.